AUS DEM LEHRSTUHL FÜR PHYSIOLOGIE
PROF. DR. ARMIN KURTZ
DER FAKULTÄT FÜR MEDIZIN
DER UNIVERSITÄT REGENSBURG

THE ROLE OF LRRC8A FOR CELLULLAR VOLUME REGULATION AND APOPTOSIS

Inaugural – Dissertation
zur Erlangung des Doktorgrades
der Medizin

der
Fakultät für Medizin
der Universität Regensburg

vorgelegt von
Anna Zormpa

2015

AUS DEM LEHRSTUHL FÜR PHYSIOLOGIE
PROF. DR. ARMIN KURTZ
DER FAKULTÄT FÜR MEDIZIN
DER UNIVERSITÄT REGENSBURG

THE ROLE OF LRRC8A FOR CELLULLAR VOLUME REGULATION AND APOPTOSIS

Inaugural – Dissertation
zur Erlangung des Doktorgrades
der Medizin

der
Fakultät für Medizin
der Universität Regensburg

vorgelegt von
Anna Zormpa

2015

Dekan:	Prof. Dr. Dr. Torsten E. Reichert
1. Berichterstatter:	Prof. Dr. Karl Kunzelmann
2. Berichterstatter:	Prof. Dr. Bernhard Weber
Tag der mündlichen Prüfung:	15.03.2016

Table of contents

1. Deutsche Zusammenfassung/ German Summary

Volumenregulation stellt eine überlebenswichtige Eigenschaft aller Zellen dar und spielt bei mehreren physiologischen und pathologischen Vorgängen eine Rolle. Der volumenregulierte Anionen- Kanal (volume regulated anion channel; VRAC) ist an der Volumenregulation, genauer an der regulatorischen Volumenabnahme (regulatory volume decrease; RVD), sowie an der Volumenabnahme während der Apoptose (apoptotic volume decrease; AVD) beteiligt. Das Protein LRRC8A (leucin rich repeat protein 8A) wurde vor kurzem als essenzielle Komponente von VRAC identifiziert.

Die Rolle von LRRC8A bei der RVD von HeLa Zellen konnte in der vorliegenden Arbeit mit Methoden der Durchflusszytometrie bestätigt werden. Das Herunterregulieren der Expression von LRRC8A durch RNA Interferenz und die pharmakologische VRAC Hemmung führten zu einer verzögerten RVD, hoben aber die RVD nicht auf. Es zeigte sich, dass andere Transportmechanismen, wie der K^+-Cl^- Symporter (KCC), eine entscheidende Rolle spielen. Trotz der universellen Expression des LRRC8A Proteins, trägt dieses in verschiedenen Zelltypen in unterschiedlichem Maße zur RVD bei. In der vorliegenden Arbeit sollte auch geklärt werden, ob Ca^{2+} aktivierte Chlorid-Kanäle der TMEM16 Familie an der RVD beteiligt sind. Die Ca^{2+} aktivierten Chlorid-Kanäle TMEM16F- und TMEM16K-Proteine hatten keinen direkten Effekt auf die RVD von HeLa Zellen.

Auf die Proliferation von HeLa Zellen hatte die Expression des LRRC8A Proteins keinen Effekt. Das Herunterregulieren der Expression von LRRC8A und die pharmakologische Hemmung von VRAC konnten die AVD nicht inhibieren. Die vorliegenden Daten deuten darauf hin, dass KCC und TMEM16F an der AVD beteiligt sind.

2. Introduction

2.1 Cell volume regulation

Cell volume regulation is an extremely important cellular function, as it is involved in a variety of physiological and pathological procedures, such as epithelial transport, regulation of metabolism, proliferation, differentiation, migration, necrosis and apoptosis. Water can easily pass through the cell membrane via water channels called aquaporins (AQP). The cell membrane is much less permeable to ions ; sodium (Na^+), potassium (K^+), calcium (Ca^{2+}) and chloride (Cl^-) ions can only pass through ion channels and ion pumps, whereas large negatively charged polyvalent macromolecules are practically confined in the intracellular compartment. Thus, a change of the extracellular osmolality leads to an initial rapid influx or efflux of water because of the osmotic dysequilibrium of water across the cell membrane. When the cell is exposed to decreased extracellular osmolality, water rapidly enters through the plasma membrane and causes cell swelling and subsequent activation of channels or transporters, which release K^+, Cl^- and small organic osmolytes from the cell. Due to osmotic pressure water molecules are obliged to follow, leading to decrease of the cell volume, a process called regulatory volume decrease (RVD) (Wehner et al. 2003) (Fig.1).

2.2 Regulatory volume decrease

RVD is mediated through swelling activated Cl^- and K^+ channels as well as K^+-Cl^- cotransporters. Before molecular identification of these channels, the ion efflux (current) had been described phenomenologically by electrophysiological methods. Further research could then correlate the swelling activated K^+ efflux [K^+ current, $I_{K+(VOL)}$] with Ca^{2+} activated K^+ channels of large (BK), intermediate (IK) and , to lesser extent, small conductance (SK), as well as with voltage gated K^+ channels (Kv1, Kv4), tandem pore domain (2P-4TM) and KCNQ K^+ channels (Stutzin und Hoffmann 2006). The K^+-Cl^- cotransporters (KCC), a subfamily consisting of four homologues, has been found to be the mediator of the swelling activated coupled K^+ and Cl^- efflux (Dunham et al. 1980; Lauf und Adragna 2000). On the contrary, things turned out to be much more complicated regarding the swelling activated Cl^- current [$I_{Cl(swell)}$]. Even though this current could be recorded as early as 1988 (Hazama und

Okada 1988) and the biophysical properties of its channel could be characterized extensively (Hoffmann et al. 2009), its molecular identity had been elusive for almost thirty years. This channel is known as volume regulated anion channel (VRAC) but, because of its properties, has also received the names volume sensitive outwardly rectifying anion channel (VSOR) or volume sensitive organic osmolyte and anion channel (VSOAC).

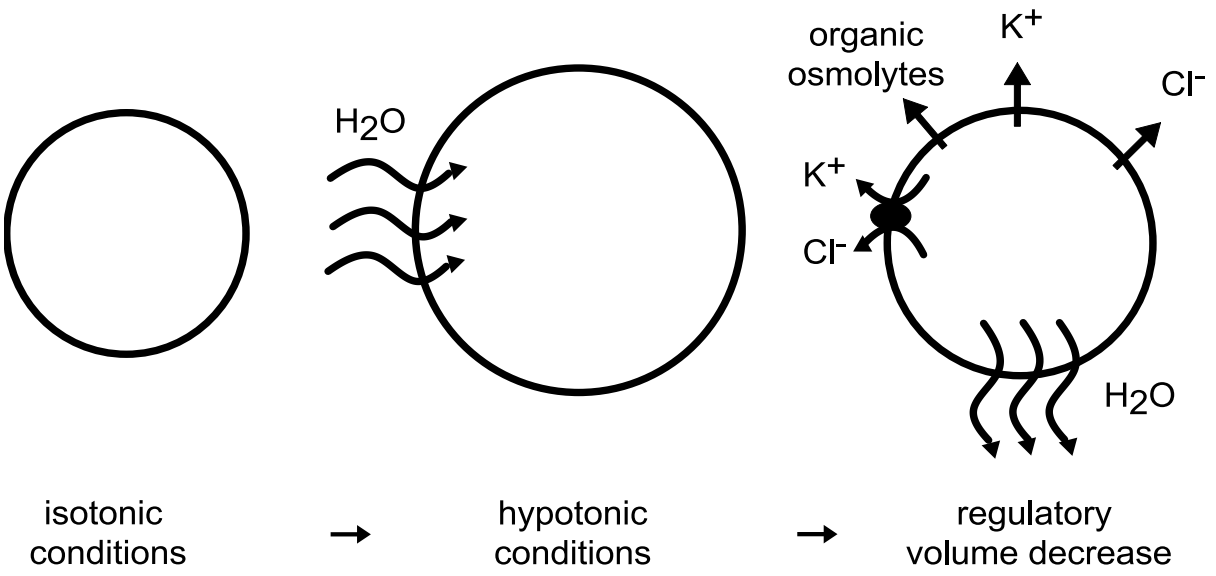

Figure 1: Mechanism of regulatory volume decrease. Hypotonic challenge osmotically drives H_2O into the cell, causing it to swell. After channel or transporter activation, K^+, Cl^- and small organic osmolytes are released from the cell, followed by H_2O.

2.3 VRAC characteristics and identification

Although cell swelling is the main mechanism of VRAC activation, it has been demonstrated that a reduction in the intracellular ionic strength also leads to VRAC activation even under isovolumetric conditions (Nilius et al. 1998). The VRAC current has been described as outwardly rectifying, meaning that the channel more easily transfers anions in the outward direction (towards the cytosolic compartment) than in the inward direction (out of the cell). VRAC can also transfer other halide ions except Cl^-, like I^-, F^- and Br^-, as well as much larger amino acids, e.g. taurine, glutamate and aspartate. VRAC exhibits a different permeability for each of those molecules, following the sequence I^-> Br^-> F^-> taurine> glutamate> aspartate (Nilius et al. 1994). The pharmacological properties of VRAC have been tested with a wide variety of substances; some of its inhibitors are the classic Cl^- channels inhibitors 4,4'-

diisothiocy-ano-2,2'-stilbenedisulfonic acid (DIDS), 5-nitro-2-(3-phenylpropyl-amino) benzoic acid (NPPB), and niflumic acid, anti-estrogens, such as tamoxifen, the novel group of acidic di-aryl-ureas and 4-(2-butyl-6,7-dichlor-2-cyclopentyl-indan-1-on-5-yl)-oxybutyric acid (DCPIB) (Hélix et al. 2003; Han et al. 2014). Nevertheless, none of them has been shown to be potent and perfectly selective, a fact which has also impeded the identification of VRAC.

Several proteins have been proposed as potential VRAC candidates over the last years, more recently including TMEM16A, TMEM16F and bestrophins. Nevertheless, none of them exhibited all of the VRAC properties (Pedersen et al. 2015). The elusive channel seems to have been identified in 2014 by two independent groups. Qiu et al. (Qiu et al. 2014) and Voss et al. (Voss et al. 2014) have simultaneously reported that the leucin rich repeat protein 8A (LRRC8A)/ SWELL 1 is an essential component of VRAC. LRRC8 is a protein family consisting of five members, LRRC8A-LRRC8E, which was first described in a girl with agammaglobulinemia (Sawada et al. 2003). Both groups claim that LRRC8A is a broadly expressed cell membrane protein which is indispensable for VRAC currents. The other four isoforms are thought to be dispensable, but the generation of VRAC current requires at least the presence of one of them in the cell in combination with LRRC8A (Qiu et al. 2014; Voss et al. 2014). LRRC8A mediated currents were shown to be involved in RVD in HeLa cells (Qiu et al. 2014). A sequence resemblance to the family of pannexins has been observed, possibly suggesting an organization of LRRC8 subunits in hexamers, as pannexins (Abascal und Zardoya 2012).

2.4 Role of VRAC in apoptosis

Apoptosis, a form of programmed cell death, is a tightly regulated complex procedure, which plays an important role in physiological and pathological processes, such as organ development, cell turnover and cancer (Kerr et al. 1972). Two major apoptotic pathways have been identified: the extrinsic-death receptor pathway and the intrinsic-mitochondrial pathway. They both have the subsequent activation of the executioner caspase 3 in common, which then leads to protease and endonuclease activation, resulting to chromatin and cytoplasmic condensation, DNA fragmentation, cytoskeleton degradation and apoptotic bodies formation. The subsequent phagocytosis of the apoptotic bodies effectively eliminates the cell residues without

causing an inflammatory response (Elmore 2007). A morphological hallmark of apoptosis is an initial cell shrinkage, called apoptotic volume decrease (AVD). AVD is, similar to RVD, the result of K^+ and Cl^- efflux. Apoptotic stimuli, apart from osmotic swelling, have been shown to activate the VRAC, leading to Cl^- efflux and AVD in many different cell types (Okada et al. 2006). VRAC inhibition has been reported to abolish AVD after pharmacological induction of apoptosis and, further, to inhibit apoptosis. From this assays was concluded that AVD is a prerequisite for apoptosis (Maeno et al. 2000).

Furthermore, cisplatin induced apoptosis was associated with enhanced VRAC activity in cancer cells (Okada et al. 2006; Cai et al. 2015) and consecutive studies reported that acquired cisplatin resistance in cancer cells is linked to impaired VRAC activity (Lee et al. 2007; Sørensen et al. 2014).

2.5 Role of TMEM16 in RVD and apoptosis

TMEM16 is a novel family of 10 proteins, also known as anoctamins. Whereas TMEM16A and TMEM16B have been functionally characterized as Ca^{2+} activated Cl^- channels (CaCC) with roles in transepithelial ion transport, smooth muscle contraction, olfaction, phototransduction, pain perception and cell proliferation, the function of the other members still remains an object of intensive research (Tian et al. 2012; Picollo et al. 2015). TMEM16F has been described to act as a CaCC (Schreiber et al. 2010), as a cation channel (Yang et al. 2012) and as a phospholipid scramblase (Suzuki et al. 2010), transporting phospholipids between the two leaflets of the cell membrane. To date it remains unclear how TMEM16F can combine those heterogenous features.

An uneven distribution of phospholipids in the two layers of the cell membrane is essential for cell homeostasis. The phospholipid phosphatidylserine also shows an uneven distribution, being located only on the inner leaflet of the cell membrane in resting cells (Verhoven 1995). Loss of this asymmetry with appearance of phosphatidylserine on the outer membrane activates the haemostasis cascade (Lentz 2003) and the apoptotic pathway and is also essential for the phagocytic recognition of apoptotic cells by macrophages (Fadok et al. 2001). The activity of TMEM16F as a scramblase and a channel has been shown to contribute to haemostasis as well as to apoptosis (Yang et al. 2012; Kmit et al. 2013).

Recently TMEM16K has been reported to augment RVD in macrophages (Hammer et al. 2015).

2.6 Purposes of the present study

VRAC is involved in the processes of regulatory and apoptotic volume decrease, thus playing an important role in cell volume regulation and apoptosis. VRAC has been chosen as the topic of this study because of its significance for a number of pathological conditions, including cancer and acquired resistance to chemotherapeutics, and, thus, for its clinical importance. The molecular identity of VRAC has been unknown for decades and recently Qiu et al. and Voss et al. claimed to have identified the protein LRRC8A as its essential component. The objective of this study was to confirm or disprove the proposed role for LRRC8A in the RVD. The RVD was principally examined in HeLa cells, one of the cell models used by the two groups mentioned above, and further in BHY cells, after VRAC inhibition or LRRC8A knockdown. A further goal of this study was to investigate the role of LRRC8A/ VRAC in apoptosis. In this case, apoptosis was induced chemically after pharmacological VRAC inhibition or LRRC8A knockdown and the apoptosis rate was assessed with caspase 3 assays. Additionally, the role of the TMEM16 proteins in RVD and apoptosis was examined using the same methodology.

3. Materials and methods

3.1 Cell culture

The cell lines used were the cervical adenocarcinoma cell line HeLa, provided by Prof. Dr. Karin Hoppe-Seyler (German Cancer Research Center, Heidelberg) and the oral squeamous cell carcinoma cell line BHY, provided by Dr. Christian Ruiz (Institute of Pathology, University Clinic, Basel). HeLa cells were cultured in Dulbecco's modified Eagle medium containing 1 g/L D-glucose, L-glutamine and pyruvate and BHY cells were cultured in OptiMEM. Both were supplemented with 10% fetal bovine serum, 100 U/ mL penicillin and 100 µg/ mL streptomycin (all from Gibco, Life Technologies, Saint Louis, MI, USA). HeLa were passaged every 4 to 5 days and BHY every 7 days, both were cultured in T75 wells (Cellstar, Greiner Bio-One, Frickenhausen).

3.2 RNA interference

A useful method for protein function studies is carrying out experiments after eliminating the expression of the responsible gene, a procedure called gene knockdown. The product of gene transcription is the messenger RNA (mRNA), which is then translated into the protein. By inserting a synthetic RNA molecule into the cell with a sequence complementary to the mRNA of interest, the two molecules bind together and are degradated, thus hindering translation and protein expression. This small RNA molecule is called small interfering RNA (siRNA), its insertion into the cell is called transfection and the whole process is called RNA interference. In order to insert the siRNA into the cell through the, under normal conditions impermeable for nucleic acids, plasma membrane, two methods of transfection were used; lipofection and electroporation. For lipofection the siRNA was embedded into vesicles made of a phospholipid bilayer, which could fuse with the cell membrane releasing their content into the intracellular compartment. For electroporation a strong electric field was used to create short-lived small water filled 'holes', through which the hydrophilic siRNA could pass the membrane.

For the transfection with siAQP3 $6x10^6$ cells were electroporated (voltage: 1005 V, width: 35 ms, pulses: 2) with 1 µL siRNA in 100 µL resuspension buffer R (Neon

Transfection System and 100 µL Neon Kit, Invitrogen, Life Technologies). The cells were then resuspended in medium without antibiotics. All other transfections were performed with lipofection using Lipofectamine 3000 (Invitrogen, Life Technologies), according to manufacturer's protocols. The final siRNA concentration in the well was 17,6 nM, the final Lipofectamin 3000 concentration was 0,16%. The cells had been seeded 12-24 hours prior to transfection in medium without antibiotics.

After transfection the cells were incubated for 24-72 hours before being used for experiments, according to the time point of the best protein suppression in immunoblotting. For the transfection with siTMEM16F, siTMEM16K and siAQP3 we used a mixture of two different siRNAs in equimolar concentration, which had been previously shown in immunoblotting to suppress the protein expression better compared to a single siRNA. All siRNAs used were purchased from Ambion, Life Technologies. Their sequence is shown in table 1.

Table 1: Used siRNAs and their sequence.

siRNA	Sequence 5'→3'	Product type
Sicontrol	s: UAACGACGCGACGACGUAAtt as: UUACGUCGUCGCGUCGUUAtt	Silencer select
siLRRC8A	s: CCAAGCUCAUCGUCCUCAAtt as: UUGAGGACGAUGAGCUUGGtg	Silencer select
siTMEM16F	a. s: CCUGAUAUUGGUGGCAAGAUCAUAA as: UUAUGAUCUU GCCACCAAUA UCAGG b. s: CCUCCAUCAUCAGCUUUAUAAUUAU as: AUAAUUAUAA AGCUGAUGAUGGAGG	Stealth siRNA
siTMEM16K	a. s: CGAUGAGUGUUAUAUCUGU as: ACAGAUAUAA CACUCAUCG b. s: GAAUCGUCUCUAUCGAUAU as: AUAUCGAUAG AGACGAUUC	Silencer select
siAQP3	a. s: GGACACUUGGAUAUGAUCA as: UGAUCAUAUCCAAGUGUCC b. s: CCGGCAUCUUUGCUACCUA as: UAGGUAGCAA AGAUGCCGG	Silencer select

3.3 RNA isolation and reverse transcription-PCR (RT-PCR)

Total RNA was isolated from HeLa cells using NucleoSpin RNA Kit (Macherey-Nagel GmbH, Düren). Complementary DNA (cDNA) was prepared in a total volume of 50 µl. Total RNA (1 µg) was denaturated at 70°C for 5 min and was hybridized to random primers (500 ng) at 21°C for 10 min. Reverse transcription occurred at 40°C for 1 hour in the presence of 200 Moloney murine leukemia virus reverse transcriptase (UM-MLV RT), 40 U of RNasin ribonuclease inhibitor, 500 µM dNTPs, in M-MLV RT 5X buffer containing 50mM Tris-HCl (pH 8.3), 75mM KCl, 3mM $MgCl_2$ and 10mM DTT. Finally, the RT was inactivated at 70 C for 15 min. PCR was performed in a total volume of 20 µL containing 0,5 µL of the reverse transcription reaction, 0,2 mM dNTPs, 1 µL of each primer (10 µM, Eurofins MWG Operon, Huntsville, AL, USA) and 0,5 U Go Taq G2 DNA polymerase and Go Taq reaction buffer with 1,5 mM $MgCl_2$. PCR consisted of a denaturizing step of 2 min at 95 °C followed by 30 cycles of 30 s in 95 °C, 30 s in 58 °C and 1 min in 72 °C. Unless stated otherwise, everything was purchased from Promega (Madison, WI, USA). The primers used for PCR are listed in table 2.

Table 2: Primers used in the RT-PCR.

Target	Sequence(5'→3')	Annealing temperature	Size (bp)
TMEM16A	s: CGACTACGTGTACATTTTCCG as: GATTCCGATGTCTTTGGCTC	62 °C 60 °C	445
TMEM16B	s: GTCTCAAGATGCCAGGTCCC as: CTGCCTCCTGCTTTGATCTC	64 °C 62 °C	553
TMEM16C	s: CTTCCCTCTTCCAGTCAAC as: AAACATGATATCGGGGCTTG	58 °C 58 °C	461
TMEM16D	s: CGGAAGATTTACAGGACACCC as: GATAACAGAGAGAATTCCAATGC	64 °C 64 °C	503
TMEM16E	s: GAATGGGACCTGGTGGAC as: GAGTTTGTCCGAGCTTTTCG	58 °C 60 °C	713
TMEM16F	s: GGAGTTTTGGAAGCGACGC as: GTATTTCTGGATTGGGTCTG	60 °C 58 °C	325

TMEM16G	s: CTCGGGAGTGACAACCAGG as: CAAAGTGGGCACATCTCGAAG	62 °C 64 °C	470
TMEM16H	s: GGAGGACCAGCCAATCATC as: TCCATGTCATTGAGCCAG	60 °C 54 °C	705
TMEM16I	s: GCAGCCAGTTGATGAAATC as: GCTGCGTAGGGTAGGAGTGC	56 °C 62 °C	472
TMEM16K	s : GTGAAGAGGAAGGTGCAGG as: GCCACTGCGAAACTGAGAAG	60 °C 62 °C	769
LRRC8A	s: CGCAGATAGCAGAGCCATCC as: CATCTTGCTGAAGGCCGGC	64 °C 62 °C	603

The PCR products were separated using a 2% agarose (Biozym Scientific, Hessisch Oldendorf) gel electrophoresis. The RNA isolation, reverse transcription and PCR were performed at least in triplicate.

The mRNA expression levels of the examined proteins were normalized to GAPDH using the program MetaMorph (Universal Imaging Corporation, New York, USA).

3.4 Proliferation assays

HeLa cells were seeded in a density of 10.000 cells/ ml DMEM+10% FBS well in 24-well-plates (TPP, Trasadingen, Switzerland). The transfection with siLRRC8A was performed 12 hours later. The cells were treated with the compounds DMSO 0,1%, tamoxifen 1 µM and 10 µM (both from Sigma-Aldrich) and T16inh-A01 10 µM (Tocris Bioscience, Bristol, UK). In the compound treated group the initial media was removed and replaced with media containing the compound in the desired concentration 12 hours post seeding. A change of media was performed in the compound group every 24 hours. The cell numbers/ well were count in a triplicate for seven days, starting 24 hours post seeding (day 1). For counting, cells were detached from the well as following: the medium was removed; after a washing step with Dulbecco's phosphate-buffered saline containing $CaCl_2$ and $MgCl_2$ ($DPBS^+$) (Gibco), cells were incubated with 1 mM EDTA-DPBS for 5 minutes. EDTA (ethylenediaminetetraacetic acid) was also purchased from Gibco. Supernatant was removed and cells were incubated with 0,5 ml trypsin (Gibco). Five minutes later, DMEM+10% FBS (0,5 ml) was added and cells were transferred for measurement to a 1,5 ml tube (Eppendorf, Wesseling-Berzdorf).

3.5 Flow cytometry

Cell volume, number and viability were measured with flow cytometry using Casy Model TT Cell Counter and Analyser (Roche, Indianapolis, Indiana, USA) relying on electronic pulse area analysis and on electric current exclusion principle respectively. According to manufacturer's instructions the cell sample was diluted in an isotonic saline solution (Casy Ton, Roche) and was aspirated with a constant speed into a capillary with a narrow measuring pore. An electrical field was applied into the measuring pore. Generally the viable cells passing through the pore have an intact cell membrane, which generates an increased resistance, compared to the electrolyte solution. This increased resistance is detected by the flow cytometer and serves as a dimension for cell size. On the contrary, dead cells have a permeable to electrical current membrane, but an impermeable nucleus, leading to the recording of smaller resistance, which is interpreted as a smaller cell diameter (Fig. 2).

Initially we examined the distribution of cells growing exponentially and the distribution of cells after induction of cell death. In this manner it was possible to identify the size of the nucleus and set it as a threshold to differentiate between viable and dead cells in the upcoming measurements (Fig. 3). The particles with a very small size were interpreted as debris. We repeated this procedure for HeLa and BHY cells and created two different set-ups for the upcoming experiments. The size of HeLa and BHY cells was found to be between 15-20 µm, so the 150 µm capillary was selected for the experiments, according to manufacturer's instructions. For the proliferation experiments we adjusted the dilution factor (volume of cell suspension/ volume of CASY ton) in such a way, that the total cell count was higher than 1000 pro measurement to guarantee statistically reliable results.

Experiments regarding cell proliferation were carried out at room temperature (RT) using filtered (Minisart filter 0,45 µm, Sartorius stedim, Göttingen) Casy Ton. The experiments concerning the RVD were carried out at 37°C in Ringer's solution (290 mOsm/ kg), hypotonic 35% Ringer' s solution (depletion of 50 mM NaCl, 210 mOsm/ kg) and isotonic Ringer's solution (50 mM NaCl replaced with mannitol, 290 mOsm/ kg) (Table 3). All solutions apart from Casy Ton were initially filtered with a Nalgene

Rapid-Flow filter (Thermo-Fischer Scientific, Waltham, MA USA). Before use they were additionally filtered with a 0,45 µm Minisart filter.

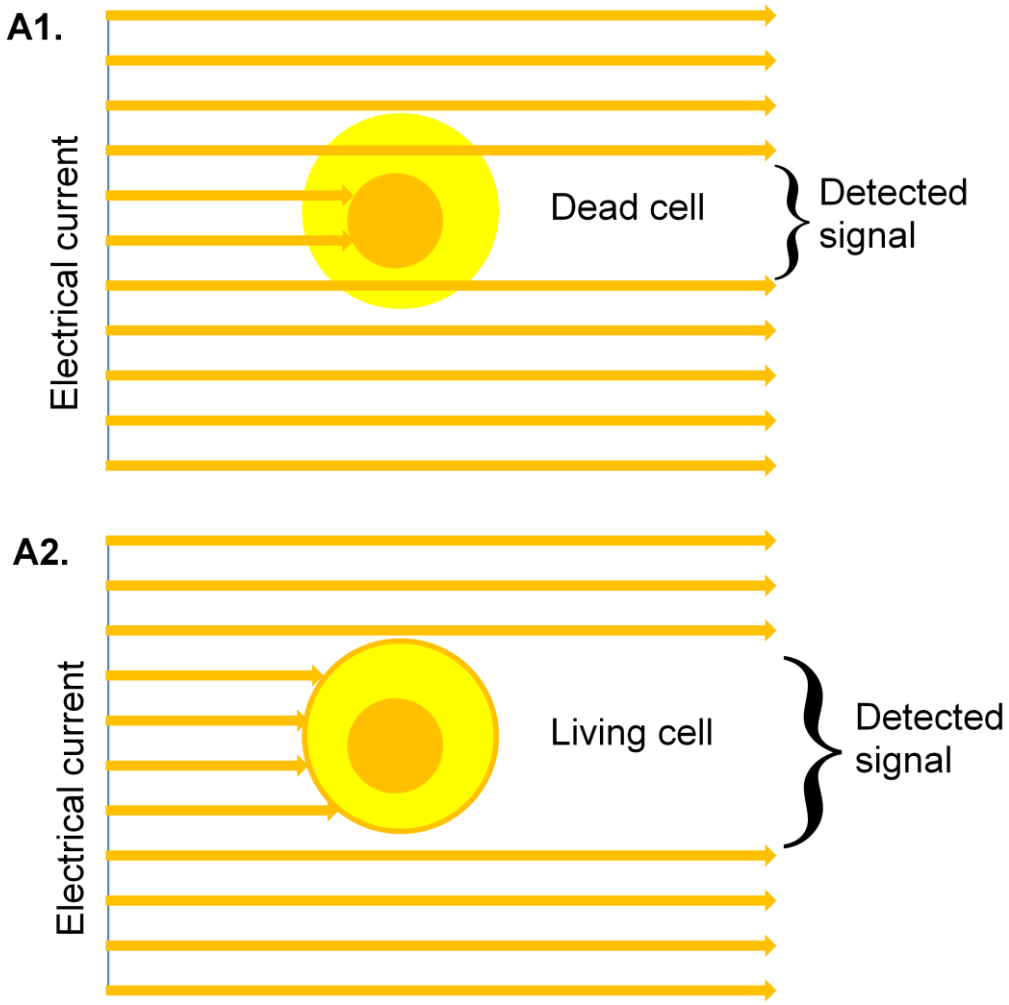

Figure 2: CASY cell counter: electric current exclusion principle. A1. Dead cells have a cell membrane permeable to the electrical current. The signal detected represents the size of the nucleus. A2. Living cells have an intact membrane which is impermeable to the electrical current. The detected signal refers to the cell size.

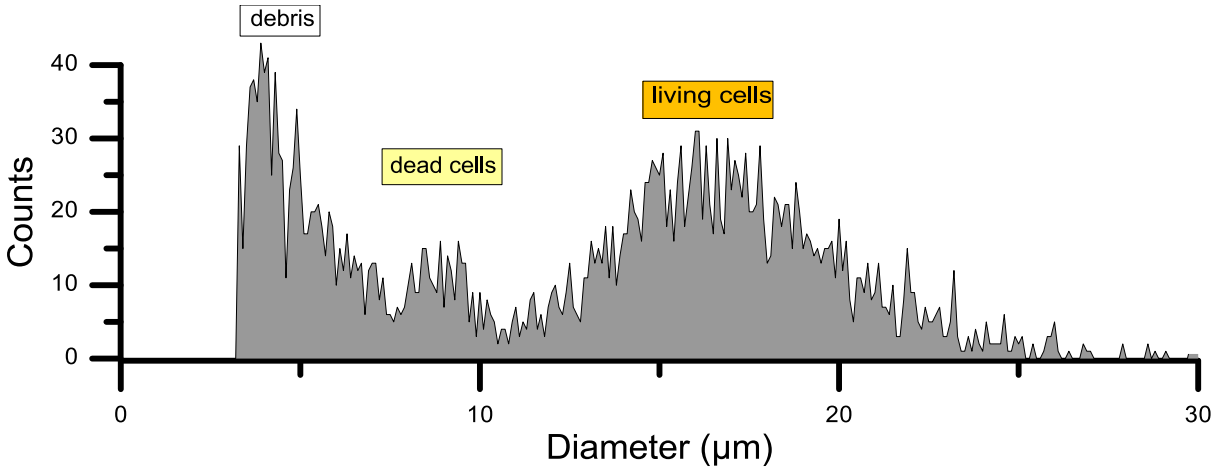

Figure 3: Casy cell counter. Typical size distribution of HeLa cells growing exponentially.

Table 3: Used solutions. Molar concentrations of compounds given in mmol/ L. The pH of the solutions was corrected to be 7,4 with NaOH or HCl prior to their use.

	Ringer's	Ringer's -50mM NaCl/ isotonic	Ringer's -50 mM NaCl/ hypotonic 35%
NaCl	145	95	95
KH_2PO_4	0,4	0,4	0,4
$K_2HPO_4.3\ H_2O$	1,6	1,6	1,6
Glucose	5	5	5
$MgCl_2.6H_2O$	1	1	1
Ca-Gluconate.$1H_2O$	1,3	1,3	1,3
Mannitol		100	
Osmolality (mOsm/ kg)	290	290	210

3.6 RVD experiments

Initially the size of polystyrene beads (20 µm, Polysciences Inc., Warrington, PA, USA) was measured in Ringer's and Ringer's -50 mM hypotonic 35% solution. In this way it could be ruled out that the different tonicity influences the recorded size (data not shown).

3.6.1 Seeding density and incubation time

For RVD experiments in cells treated with siRNA against LRRC8A, HeLa cells were seeded in 12-well-plates in a density of 50.000 cells/ml DMEM+10%FBS and BHY cells in 12-well-plates in a density of 80.000/ ml OptiMEM+10% FBS. They were transfected after 12 hours with siRNA against LRRC8A. The RVD experiment was carried out 60 hours post transfection. For measurements of RVD in TMEM16F downregulated cells, HeLa cells were seeded at a density of 80.000 cells/ ml DMEM+10%FBS and were transfected with siRNA against TMEM16F 24 hours later. The experiment was carried out 24 hours post transfection. For RVD in TMEM16K downregulated cells, HeLa cells were seeded at a density of 80.000/ ml DMEM+10%FBS and were transfected with siRNA against TMEM16K 12 hours later. The experiment was carried out 36 hours post transfection.

For RVD experiments in cells treated with siRNA against AQP3 HeLa cells were electroporated, seeded at a density of 50.000/ ml DMEM+10%FBS and examined 72 hours post transfection. For all the experiments referred above, a control group of cells was transfected with scrambled control siRNA, all other conditions being the same. For all experiments with compounds, HeLa cells were seeded at a density of 40.000/ ml DMEM+10%FBS and the experiments were carried out 72 hours later. As stated under 3.2., a different incubation time with siRNA was applied, according to the time point of the best protein suppression in immunoblotting. The cells ware seeded at different densities, in order to be about 80%-90% confluent at the time of the experiment.

3.6.2 Experimental protocol

The cells were detached from the well as following: after washing with $DPBS^{+}$, they were incubated with 300 µl accutase (Invitrogen) for 5 minutes. Then 700 µl fresh media was added and the cells were transferred to 1,5 ml tube. BHY cells were additionally incubated with 1 mM DPBS-EDTA for 5 minutes before adding accutase. After centrifugation (400 RCF, 3 minutes, 37°C) the supernatant was removed and 500 µl Ringer's solution was added. After incubation of 10 minutes at 37°C the first measurement was performed with Casy cell counter. The sample was centrifuged again under same conditions. After removing the supernatant, 475 µL of warm (37°C) Ringer's, Ringer's hypotonic 35% or Ringer's isotonic solution were added at time

point zero (t=0). Measurements were then carried out at the time points of 0,5 ,1,5 , 2,5…10,5 minutes. Between the measurements the cell sample was kept in water bath at 37°C.

3.6.3 Compounds

The compounds used for RVD experiments were: tamoxifen, R-(+)-DIOA, DMSO, NS 8593, tetraethylammonium (TEA), staurosporin (all from Sigma Aldrich), wortmannin (Invivo Gen, San Diego, CA, USA), T16Ainh-A01, SKF 96365 and GSK 650394 (all three from Tocris Bioscience), NS 3728 (Neurosearch, Hellerup, Denmark) and bariumchloride dehydrate (Merck Millipore, Billerica, MA, USA). All compounds were dissolved in DMSO and this was used as a control. The DMSO concentration in Ringer's/ Ringer's hypotonic 35%/ Ringer's isotonic solution did not exceed 0,4% v/v, which had no effect on the RVD compared to untreated cells (data not shown). With the exception of staurosporin, all experiments in presence of compounds were carried out using Ringer's, Ringer's hypotonic 35% and Ringer's isotonic solution containing the compound in the desired concentration. Staurosporin was only added in the wells.

3.6.4 Experiments with staurosporin

The bacterial alkaloid staurosporin was used to induce apoptosis. LRRC8A and TMEM16F downregulated HeLa cells were preincubated for four hours with staurosporin 1 µM before performing the RVD experiments. For the experiments with staurosporin and RDIOA or NS 3728, HeLa cells were preincubated with RDIOA 50 µM or NS 3728 10 µM for 30 minutes and then further incubated for four hours with media containing RDIOA 50 µM or NS 3728 10 µM and additionally staurosporin 1 µM.

3.7 Data analysis and statistics

The recorded values from Casy cell counter were imported into a personal computer using software Casy Excel 2.4. (Roche). The volume values at t=0,5 up to 10,5' for every single experiment with Ringer's hypotonic 35% solution were later imported into the program OriginPro 8.0 (OriginLab Corp. Northampton, MA, USA) and were further analyzed and plotted against time. In order to compare the results of the various experiments, the RVD curves were fitted into a single exponential decay

function ($y=y_0+A^{-R_0 x}$; y being the volume at any given time point x, y_0 being the initial volume at the time point =0,5' after adding Ringer's hypotonic 35% and R_0 being the exponential decay constant). The values y_0, A and R_0 were calculated for every experiment. We used following criteria to compare the RVD in the various experiments:

a. cell volume at t=2,5' after adding Ringer's hypotonic 35%

b. R_0

c. time required for the half maximal RVD.

The half maximal RVD was calculated by subtracting the volume at t=10,5' from the volume at t=0,5', dividing by 2 and adding the quotient to the volume at t=10,5'. By replacing y with this value in the equation $y=y_0+A^{R_0 x}$, we can calculate x (y_0, A and R_0 had already been calculated).

For statistical analysis paired or unpaired Student's t-test was used with a significance level of 0,05.

3.8 Caspase 3 assay

3.8.1 Method

To study apoptosis a caspase activation assay was used. The NucView 488 Caspase-3 Assay Kit was purchased from Biotium (Hayward, CA, USA). The NucView™ 488 Caspase-3 Substrate consists of the DNA-dye NucView 488 attached to the amino acid sequence Asp-Glu-Val-Asp (DEVD), which is cleaved by activated caspase 3 (Antczak et al. 2009). The attachment of the positively charged DNA dye to the negatively charged peptide leads to electroneutrality and thus, to cell membrane permeability and, at the same time, inactivates the DNA binding ability of the compound. Though enzymatic cleavage by the activated caspase 3 in apoptotic cells the positively charged DNA dye is released, it enters the nucleus, binds the DNA and fluoresces upon excitement at 488 nm (Skommer et al. 2014)

3.8.2 Experimental protocol

For the NS 3728 and RDIOA experiment HeLa cells were seeded at a density of 100.000/ml DMEM+10%FBS in 12 well plates with fibronectin (PromoCell, Heidelberg) coated 18 mm diameter cover glasses (Hartenstein, Germany). 24 hours post seeding the cells were incubated with NS 3728 10 µM or RDIOA 50 µM or

DMSO 0,5% v/v for 30 minutes. The cover glass was attached then to a chamber using silicone (Bayer, Leverkusen) and 200 µl DMEM+10% FBS containing caspase 3 substrate 2 µM, staurosporin 1 µM or DMSO 0,5% v/v (control for staurosporin) and, additionally, NS 3728 10 µM or RDIOA 50 µM or DMSO 0,1% v/v (control for RDIOA or NS 3728). For the experiment in LRRC8A deficient cells, HeLa cells were seeded at a density of 20.000/ ml DMEM+10% FBS and transfected with siLRRC8A and control siRNA 12 hours later using Lipofectamin 3000. The experiment was carried out sixty hours post transfection. For the experiment in TMEM16F downregulated cells, HeLa cells were seeded in a density of 80.000/ ml DMEM+10% FBS and transfected with siTMEM16F and control siRNA 12 hours later. The experiment was carried out 24 hours post transfection. The cover glass was attached to a chamber using silicone and 200 µL DMEM+10% FBS containing caspase 3 substrate 2 µM, staurosporin 1 µM or DMSO 0,5% v/v.

The cover glasses were kept in wet chamber in the incubator (37°C, 5% CO_2) until images were acquired six hours later with an Axiovert 200 M microscope (Zeiss, Göttingen) and an 20x objective. The excitation wavelength was 488 nm and the exposure time 200 msec. The emission fluorescence was measured at 520 nm. Four to five image fields were collected pro cover glass. Data were acquired using the software AxioVision SE64 Rel. 4.8 (Zeiss). The number of total and fluorescent cells was counted manually using the software ImageJ (National Institutes of Health, USA).The result was given as the percentage of the fluorescent to the total cells. For every experiment at least four cover glasses were used.

3.9 Immunoblotting

3.9.1 Method

Immunoblotting is a method for detecting proteins in tissue or cell samples. After cell lysis and centrifugation steps, the proteins are separated with electrophoresis according to their molecular weight. Next, the proteins are transferred onto a special membrane, where they are accessible to the primary antibody. This antibody is designed especially for the protein of interest and binds it with high affinity. A secondary antibody, tagged with the enzyme horseradish peroxidase (HRP), is then applied and binds specifically to the primary antibody. Subsequently a

chemiluminescent agent is added and it is cleaved by the HRP producing luminescence, which is proportionate to the amount of the protein contained in the sample. The luminescence is recorded on a photographic film, where the proteins are to been seen as stained bands. The procedure is performed also for a housekeeping protein, e.g. GAPDH, which is known to be expressed in stable levels in the cell and serves as control. The bands are then compared to proteins with known molecular weight, which are used as a ‘’ladder’’ in the electrophoresis. All immunoblotting experiments were kindly performed by the PhD student Ms. Podchanart Wanitchakool.

3.9.2 Experimental protocol

Protein was isolated from HeLa and BHY cells using 1% of Nonidet P-40 (Sigma-Aldrich), separated with a 8,5-12,5 % sodium dodecyl sulfate-polyacrylamide gel electrophoresis (SDS-PAGE) and transferred onto a polyvinylidene fluoride (PVDF) membrane (Immobilon-P^{SQ} Membrane, Merck Millipore, Billerica, MA, USA). The blots were developed with SuperSignal West pico Chemiluminescent Substrate (ThermoFischer Scientific, Waltham, MA, USA). The antibodies used for immunoblotting and the conditions for the experiments are shown in table 4.

Table 4: Antibodies used for immunoblotting

Protein	First antibody	Second antibody
LRRC8A	rabbit anti-LRRC8A 1:1000, Sigma Aldrich in 0,25 % BSA/ TBST at 4°C overnight	HRP-conjugated goat anti-rabbit, 1:10.000, Acris, Hiddenhausen) in 1% NFM/ TBST at room temperature (RT) for 2 hours
AQP3	goat anti-AQP3 1:250, Santa Cruz in 1% BSA/ TBST at 4°C overnight	the HRP-conjugated donkey anti goat IgG 1:2000, Santa Cruz in 3% NFM/ TBST at RT for one hour
TMEM16A	rabbit anti-DOG1/ TMEM16A 1:1000 Novus Biologicals, Cambridge, UK in 1% NFM/TBST at 4°C overnight	HRP-conjugated goat anti-rabbit 1:10.000, Acris in 1% NFM/ TBST at RT for 2 hours
TMEM16F	rabbit anti-TMEM16F 1:500, Davids Biotechnologie Regensburg in 1% NFM/ TBST at 4°C overnight	HRP-conjugated goat anti-rabbit 1:10.000, Acris in 1% NFM/ TBST at RT for 2 hours
TMEM16K	rabbit anti-TMEM16K 1:1000, Aviva, San Diego, CA, USA in 5% NFM/ PBST at 4°C overnight	HRP-conjugated goat anti-rabbit 1:10.000, Acris in 5% NFM/ PBST at room temperature for two hours
GAPDH	rabbit anti-GAPDH (FL-335:sc-25778) 1:3000, Santa Cruz in 5% NFM/ PBST at 4°C overnight	HRP-conjugated goat anti-rabbit 1:10.000, Acris in 1% NFM/ PBST at RT for 2 hours

4. Results

4.1 TMEM16 and LRRC8A mRNA expression in HeLa cells

In order to examine the expression of TMEM16 and LRRC8A mRNA in HeLa cells we performed a RT-PCR. Figure 4 shows an expression of TMEM16F and TMEM16K and a weaker expression of TMEM16D, TMEM16H and LRRC8A.

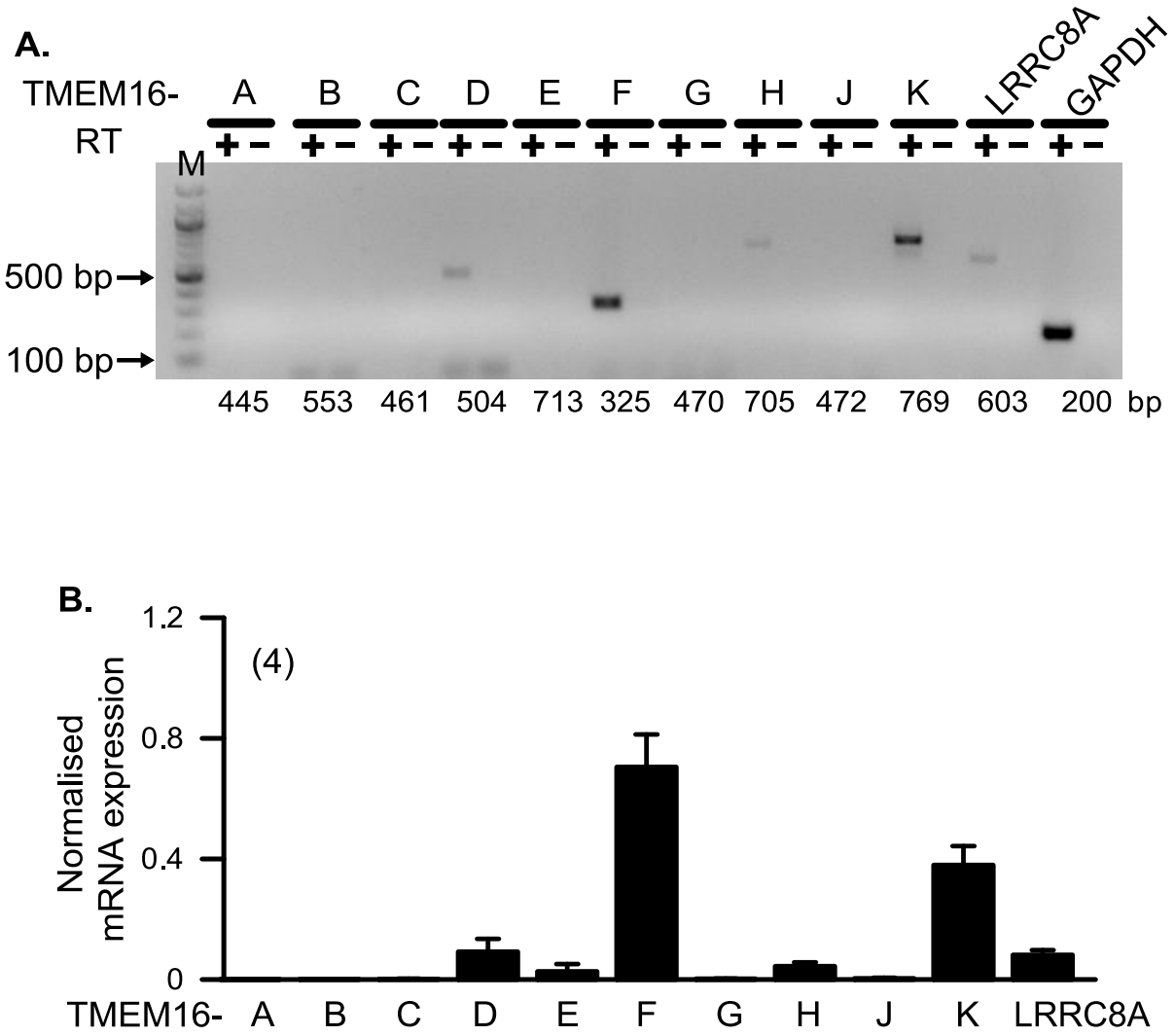

Figure 4: A. Agarose-gel electrophoresis of the reverse transcription products in HeLa cells. A. 100-base-pair (bp) DNA ladder was used as a marker (M), arrows indicate the PCR product length in base pairs (bp). RT (-) mark negative controls without use of reverse transcriptase. The length (bp) of each PCR product is stated at the bottom of the picture. B. mRNA expression levels normalized to GAPDH expression level (number of experiments).

4.2 Protein expression of TMEM16 and LRRC8A as detected by immunoblotting

As mRNA levels can significantly differ from the actual protein levels, we performed immunoblotting for TMEM16 and LRRC8A. As seen in figure 5, we could confirm the protein expression of TMEM16F, TMEM16K and LRRC8A in HeLa. We could also confirm that HeLa do not express TMEM16A. For this experiment we used the BHY cells as a positive control, as they were known from previous experiments to express TMEM16A abundantly. Further, we demonstrated that the RNA interference with siLRRC8A, siTMEM16F, siTMEM16K and si AQP3 was successful (Fig.5-6).

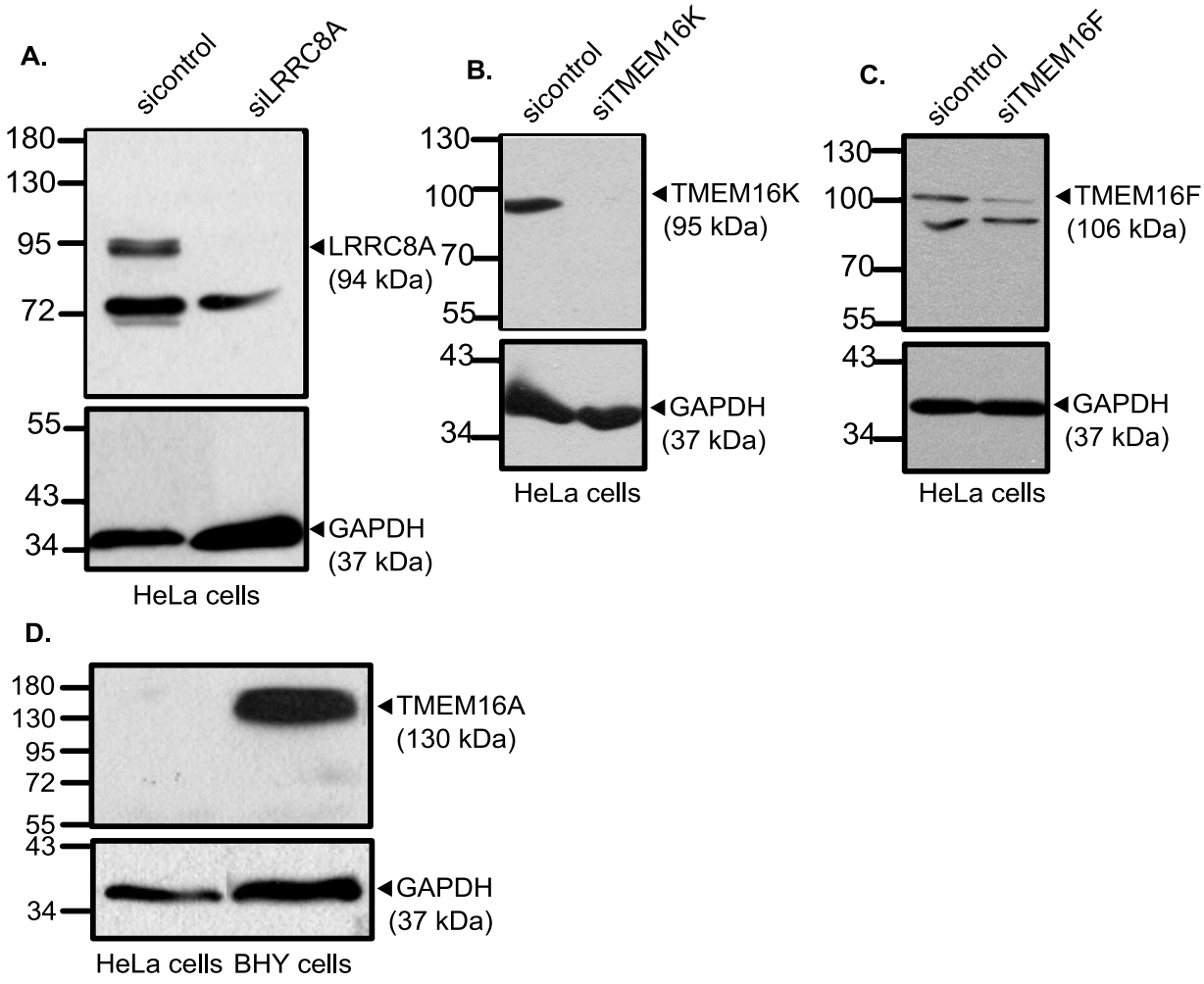

Figure 5: A. Immunoblotting of LRRC8A in sicontrol and siLRRC8A treated HeLa cells. Complete suppression after RNA interference. B. Immunoblotting of siTMEM16K in sicontrol and siTMEM16K treated HeLa cells. Complete suppression of the TMEM16K expression. C. Immunoblotting of siTMEM16F in sicontrol and siTMEM16F treated HeLa cells. Significant suppression of TMEM16F expression. D. Immunoblotting of TMEM16A in HeLa and BHY cells under control conditions. HeLa do not express detectable levels of TMEM16A, in contrast to BHY cells.

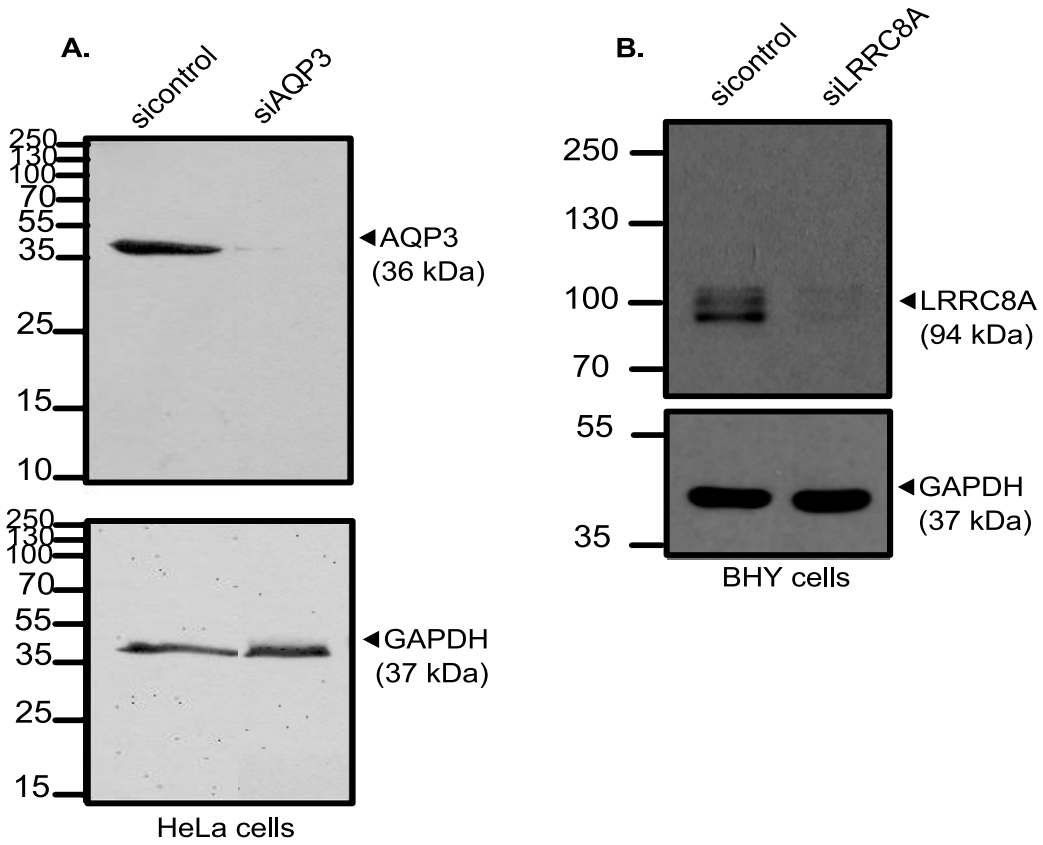

Figure 6: A. Immunoblotting of AQP3 in HeLa cells after RNA interference with siAQP3, and control siRNA showing significant protein suppression. B. Immunoblotting of LRRC8A in sicontrol and siLRRC8A treated BHY cells, showing significant protein suppression. GAPDH was used as a positive control in all experiments. The molecular weight of the protein is marked in Kilodalton (kDa) at the left of each figure.

4.3 RVD experiments

4.3.1 RVD in HeLa cells under control conditions

In the experiments depicted in figure 7 HeLa cells demonstrated a fast RVD after application of Ringer's hypotonic 35% solution at the time point zero (t_0). HeLa cells which were further kept in Ringer's control solution maintained a constant volume through the time course of the experiment. This was the case in all following experiments, so that the volume curve for Ringer's control solution will not be shown in following graphs. In order to compare the RVD efficiently among the several groups of inhibitors and after RNA interference and also independently of the initial volume in Ringer's control solution (V_0), the volume is depicted at any given time x (V) as a fraction to the initial volume (relative volume). In all further RVD experiments the cell volume will be shown as relative volume (normalized).

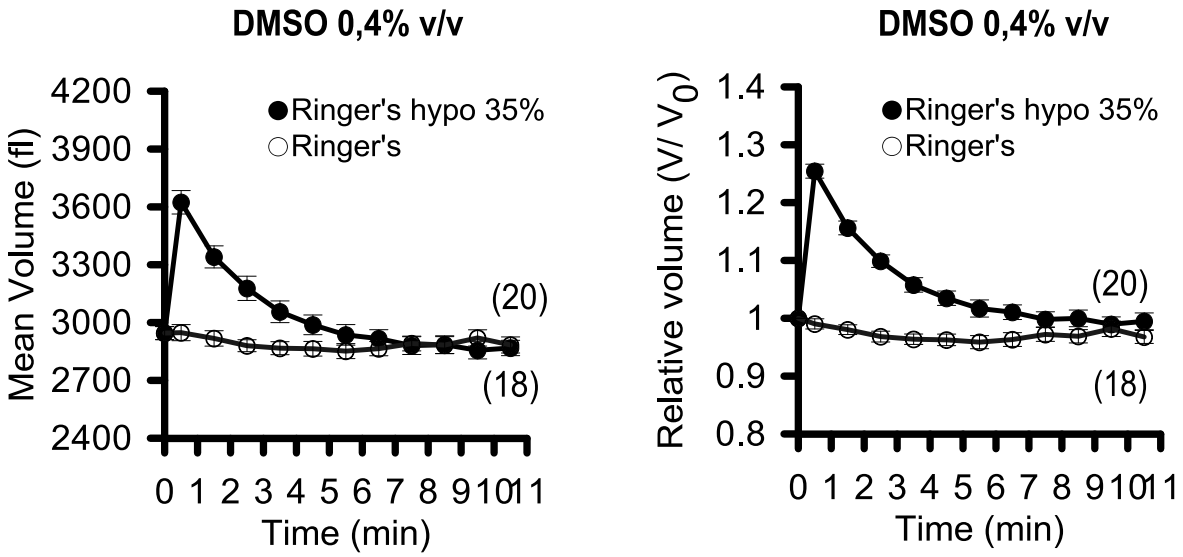

Figure 7: Volumetric response against time of HeLa cells exposed to Ringer's hypotonic 35% solution containing 0,4% DMSO v/v (closed circle) and Ringer's control solution 0,4% DMSO v/v (open circles) at t_0. A. Mean volume in fL. B. Relative volume (V/V_0). Results given as mean volume ± SEM. (Number of experiments)

All compounds used in this study were dissolved in DMSO. To rule out that the experimental results are due to the compound and not due to DMSO we used as a control group DMSO in a concentration not higher than 0,4% v/v. Addition of DMSO 0,4% v/v in Ringer's hypotonic 35% solution had no effect on the RVD compared to Ringer's hypotonic 35% only (data not shown). HeLa cells swelled to a maximal relative volume of 1,254 ± 0,012. After 2,5' the volume already reduced to 1,098 ± 0,011. The time for the half maximal RVD was 2,194 ± 0,165 seconds (s). The relative volume RVD curve shown in Fig. 7 was fitted to the equation $y = y_0 + A^{-R_0 x}$, where y_0=0,989 ± 0,004, A=0,330 ± 0,007 and R_0=0,448 ± 0,028 (adj. R-Square=0,9989).

4.3.2 RVD in LRRC8A deficient HeLa cells

Knockdown of LRRC8A lead to slightly delayed RVD response induced by Ringer's 35% hypotonic solution (Fig. 8A). The relative volume at t=2,5' was significantly higher in siLRRC8A compared to sicontrol (1,140 ± 0,019 vs. 1,074 ± 0,018) treated cells. The other criteria (R_0 and the time for half maximal RVD) were not significantly different (Fig. 16-17, see experiments without Ba^{2+}/TEA). We exchanged Ringer's solution to Ringer's isotonic solution (Table 3) and repeated the experiment. As seen in figure 8B, no significant difference could be observed between siLRRC8A and

sicontrol treated cells**.** The initial cell volume was found to be similar between control and siLRRC8A knockdown cells after incubation in control solution (Ringer's, depicted in Fig. 9, or Ringer's isotonic, data not shown) for 10 minutes. On the other hand, the initial cell volume (for both control and siLRRC8A knockdown cells) was significantly higher after incubation in Ringer's solution (3108 ± 66 fL) than in Ringer's isotonic solution containing mannitol (2702 ± 98 fL).

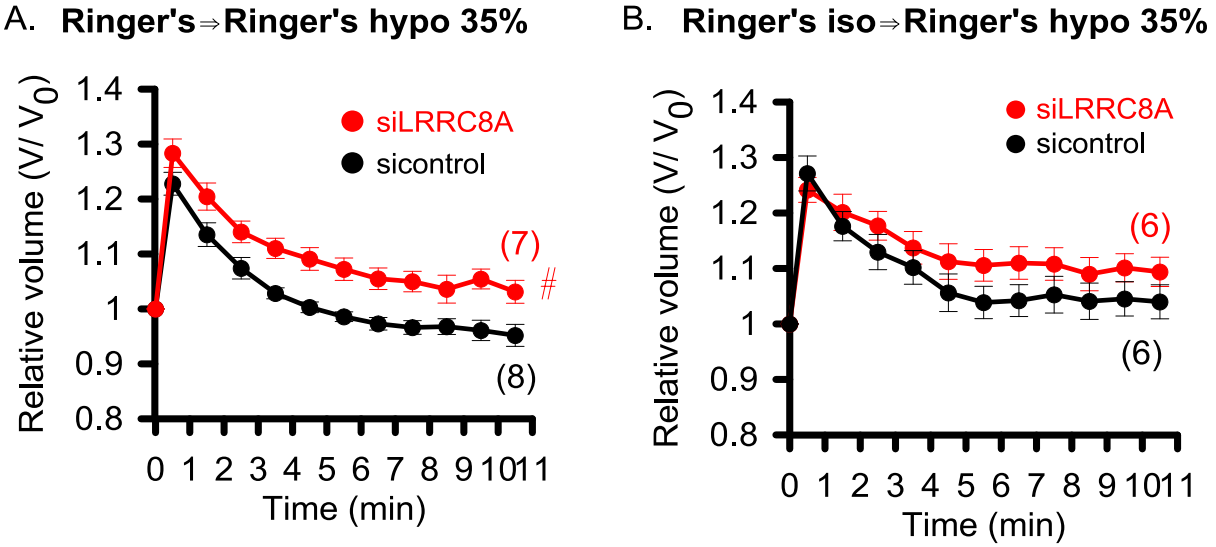

Figure 8: RVD of siLRRC8A and sicontrol treated HeLa cells. A. Preincubation with Ringer's before applying Ringer's hypotonic 35%. The relative volume at t=2,5' is significantly higher(#) in siLRRC8A compared to sicontrol. B. Preincubation with Ringer's isotonic before applying Ringer's hypotonic 35%. Results given as mean volume ± SEM. (Number of experiments**)**

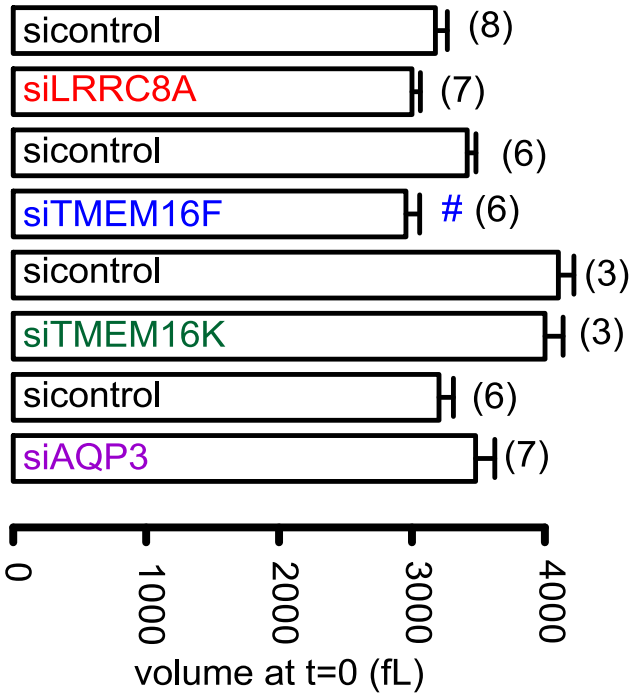

Figure 9: Initial volume at t=0 after incubation with Ringer's solution. Depicted are data for LRRC8A, TMEM16F, TMEM16K and AQP3 deficient cells and the respective sicontrol cells for each. Results given as mean volume ± SEM. (Number of experiments, common in all graphs). # significantly different from sicontrol cells.

4.3.3 RVD in LRRC8A deficient BHY cells

In order to examine if the knockdown of LRRC8A has similar effects on other cell lines, we repeated the experiment in BHY cells using the protocol Ringer's and Ringer's hypotonic 35%. BHY cells exhibited a slower RVD than HeLa cells. For this reason the measurements were performed for 15 minutes instead of 10. As shown in figure 10, the difference in the RVD response of the siLRRC8A and sicontrol treated BHY cells is more obvious than the one of HeLa cells. The time for half maximal RVD is 2.92 ± 0.348 s in sicontrol vs. 7.413 ± 0.749 s in siLRRC8A and the R_0 is 0.288 ± 0.037 and 0.074 ± 0.015 respectively. The relative volume at t=2,5' is not significantly different between the two groups, which is explained by the higher maximal volume of sicontrol and the ''flatter'' curve of siLRRC8A cells. Consistent with this, the relative volume at later time points (t=3,5'-14,5') is significantly different.

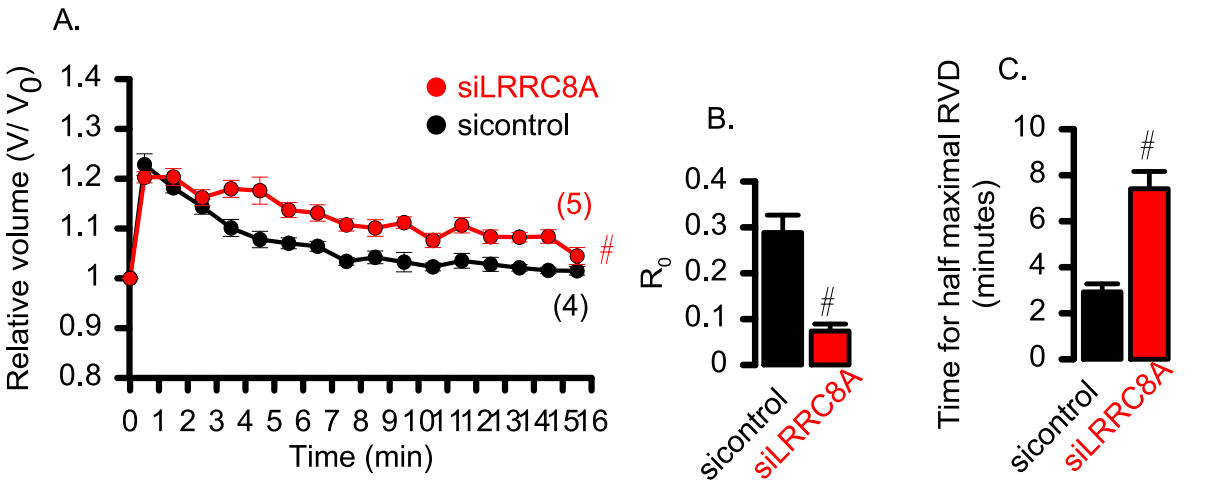

Figure 10: Effect of LRRC8A knockdown on the RVD of BHY cells exposed to Ringer's hypotonic 35%. A. Relative volume against time of siLRRC8A and sicontrol. B. # R0 is significantly higher in sicontrol than siLRRC8A. C. # Time for half maximal RVD in sicontrol is significantly shorter than for siLRRC8A. Results given as mean values ± SEM. (Number of experiments) Number of experiments is same for A.-C.

4.3.4 RVD in TMEM16 deficient HeLa cells

As LRRC8A does not evidently play a key role in the volume regulation of HeLa cells, the question emerged if the Cl^- channels family of TMEM16 is involved. As seen in figure 4, HeLa express mainly TMEM16F and TMEM16K, so we performed the RVD experiments after knockout of those proteins. Neither knockdown of TMEM16F nor of TMEM16F had an effect on the RVD (Fig. 11).

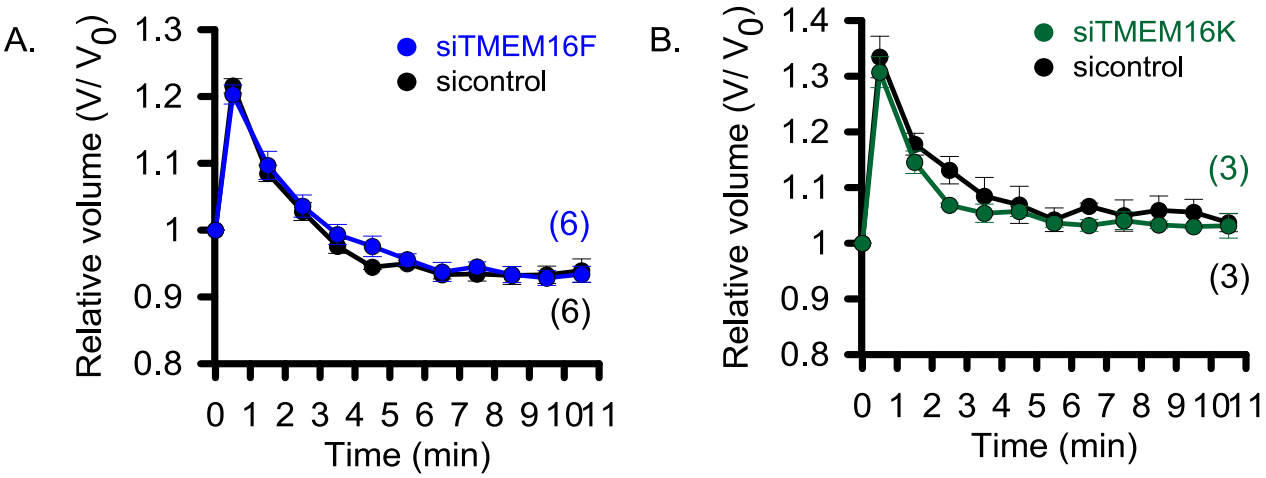

Figure 11: A. Effect of TMEM16F knockdown on the RVD of HeLa cells under Ringer's hypotonic 35% solution. B. Effect of TMEM16K knockdown on the RVD of HeLa cells under Ringer's hypotonic 35% solution. Results given as mean volume ± SEM. (Number of experiments)

4.3.5 RVD in AQP3 deficient HeLa cells

AQPs are water channels. Knockdown of AQP3 has been shown to impair RVD in human intestine epithelial cells (Kida et al. 2005). In an attempt to recognize the mechanism responsible for RVD in HeLa cells, AQP3 was also knocked down in this cell line and the RVD experiment was repeated with Ringer's and Ringer's hypotonic 35% solution. No significant change in the RVD was detected (Fig. 12).

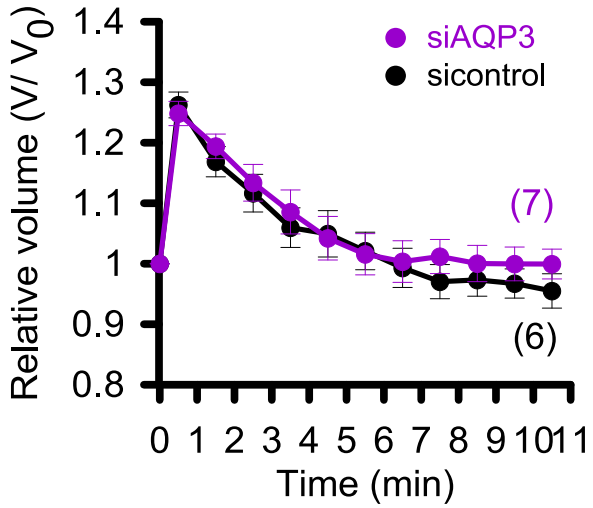

Figure 12: Relative volume against time of siAQP3 and sicontrol treated HeLa. Preincubation with Ringer's before applying Ringer's hypotonic 35% solution. Results given as mean volume ± SEM. (Number of experiments).

4.3.6 RVD in HeLa after application of Cl^- channels inhibitors

As Cl^- efflux is one of the mechanisms of RVD, several Cl^- channels inhibitors were tested for their effect on RVD of HeLa cells. Tamoxifen and NS 3728 are both VRAC inhibitors, but NS 3728 has been shown recently to block TMEM16 channels as well (Kunzelmann 2015). T16Ainh-A01 is a TMEM16 blocker.

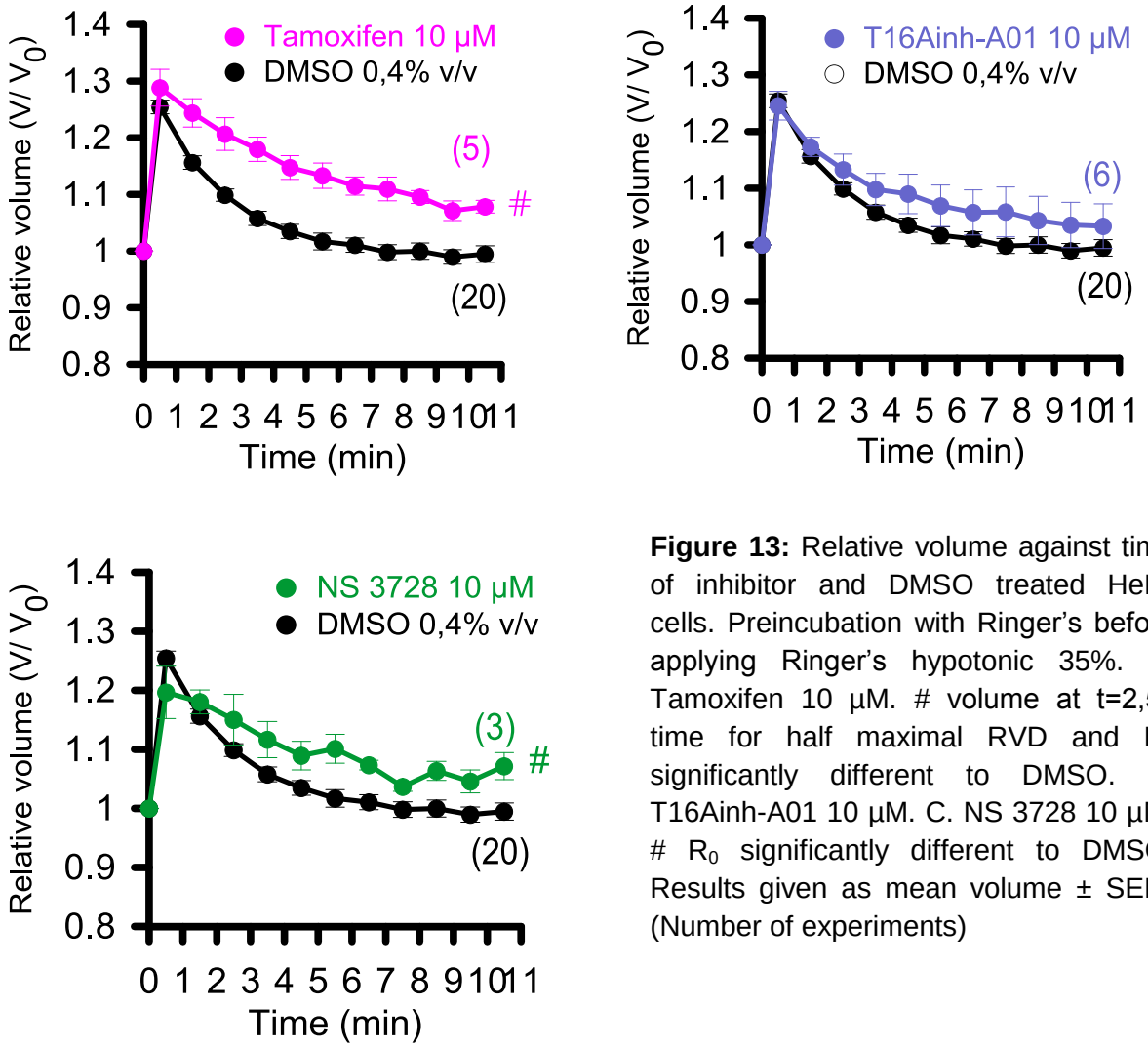

Figure 13: Relative volume against time of inhibitor and DMSO treated HeLa cells. Preincubation with Ringer's before applying Ringer's hypotonic 35%. A. Tamoxifen 10 µM. # volume at t=2,5', time for half maximal RVD and R_0 significantly different to DMSO. B. T16Ainh-A01 10 µM. C. NS 3728 10 µM. # R_0 significantly different to DMSO. Results given as mean volume ± SEM. (Number of experiments)

Tamoxifen 10 µM caused a slower RVD. Relative volume at t=2,5' (1,243 ± 0,024 vs. 1,098 ± 0,011), time for half maximal RVD (3,322 ± 0,180 vs. 2,194 ± 0,165 minutes) and R_0 (0,203 ± 0,028 vs. R0=0,448 ± 0,028) were significantly different compared to DMSO treated cells. T16Ainh-A01 had no significant effect. NS 3728 treated cells showed a flatter RVD curve (R0=0,242 ± 0,016) compared to DMSO treated cells (R0=0,448 ± 0,028) (Fig. 13).

4.3.7 RVD in HeLa after application of K^+ channels inhibitors

Ba^{2+} is a potent K^+ channel inhibitor. TEA is a nonselective antagonist of big conductance K^+ channels (BK). We performed the RVD experiments in LRRC8A, TMEM16F and TMEM16K deficient HeLa cells in the presence of 5 mM Ba^{2+} and 10 mM TEA. Ba^{2+}/TEA itself inhibited RVD significantly. The protein knockdown on the other hand showed no remarkable effect on the RVD under these conditions (Fig. 14, 15). Figures 16 and 17 quantitatively demonstrate the effect of Ba^{2+}/TEA on the criteria used to compare RVD.

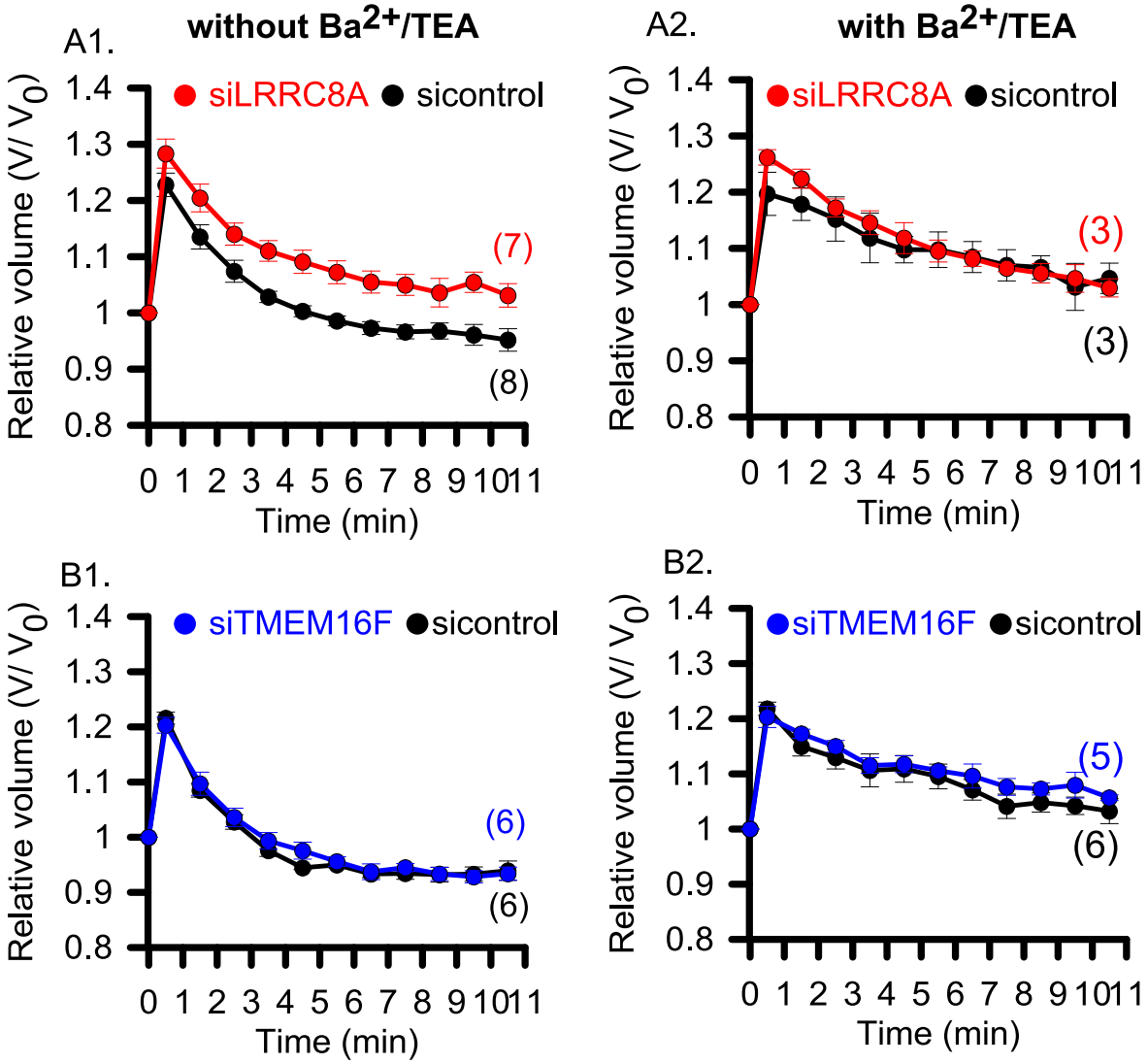

Figure 14: RVD in LRRC8A (A1) and TMEM16F (B1) deficient HeLa cells in the absence (A1, B1) and presence of Ba^{2+}/TEA (A2, B2 respectively). Preincubation with Ringer's before applying Ringer's hypotonic 35%. Results given as mean volume ± SEM. (Number of experiments)

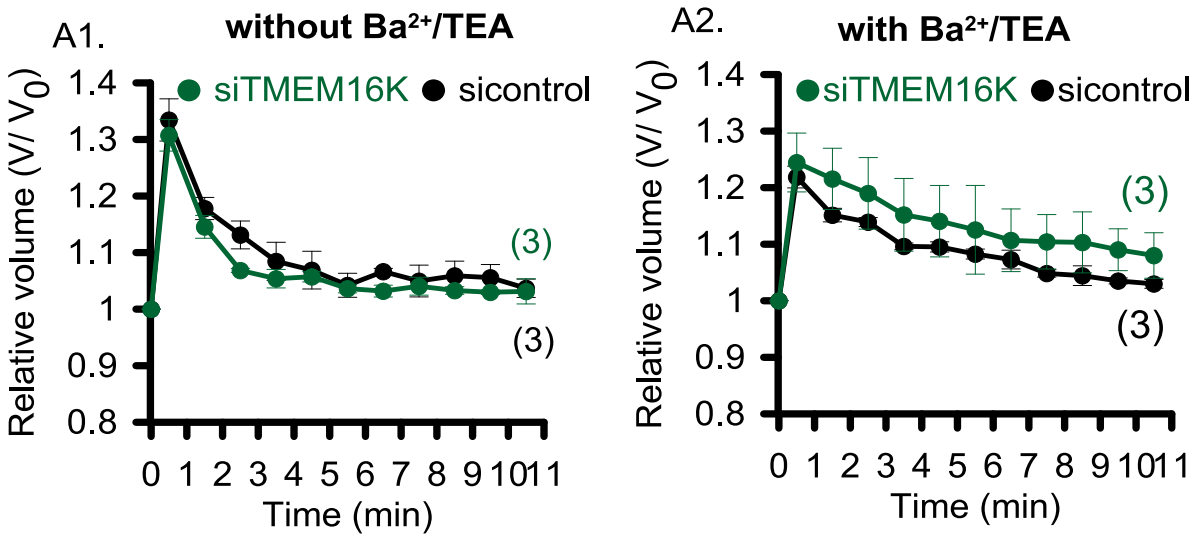

Figure 15: RVD in TMEM16K deficient HeLa cells in the absence (A1) and presence of Ba^{2+}/TEA (A2). Preincubation with Ringer's before applying Ringer's hypotonic 35%. Results given as mean volume ± SEM. (Number of experiments)

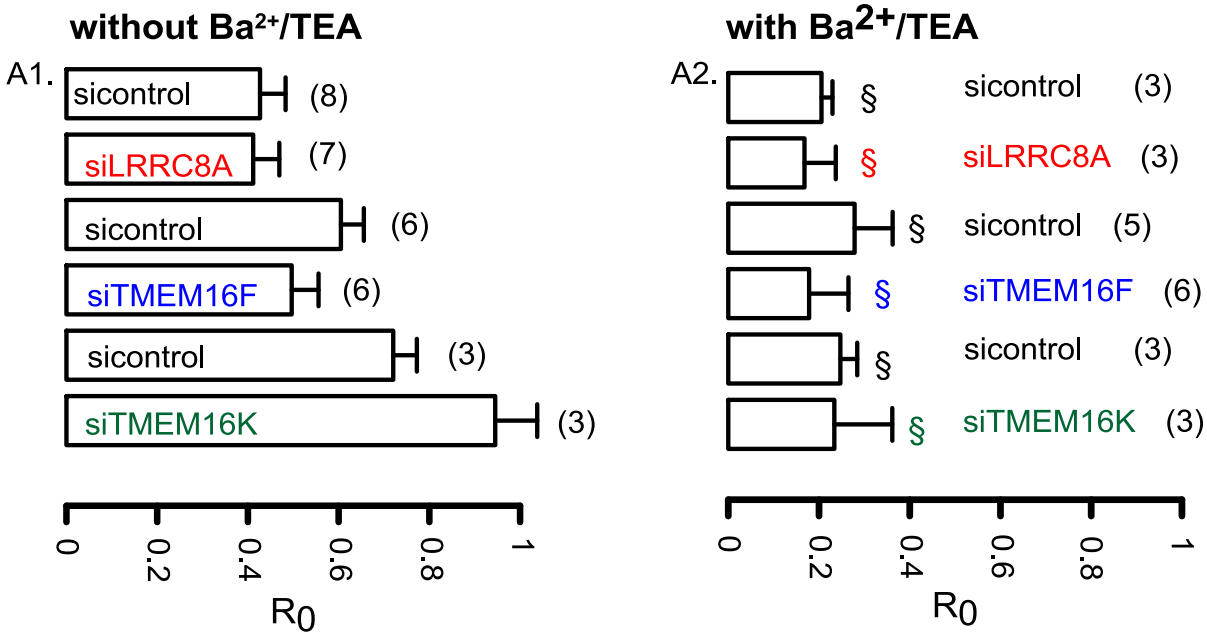

Figure 16: RVD of HeLa cells. A1. R_0 in the absence of Ba^{2+}/TEA. A2. R_0 in the presence of Ba^{2+}/TEA. R_0 significantly different (§) compared to absence of Ba^{2+}/TEA. Preincubation with Ringer's (without or with Ba^{2+}/ TEA) before applying Ringer's hypotonic 35% (without or with Ba^{2+}/TEA). Depicted are data for LRRC8A, TMEM16F and TMEM16K deficient cells and the respective sicontrol treated cells for each group. Results given as mean R_0 ± SEM. (Number of experiments)

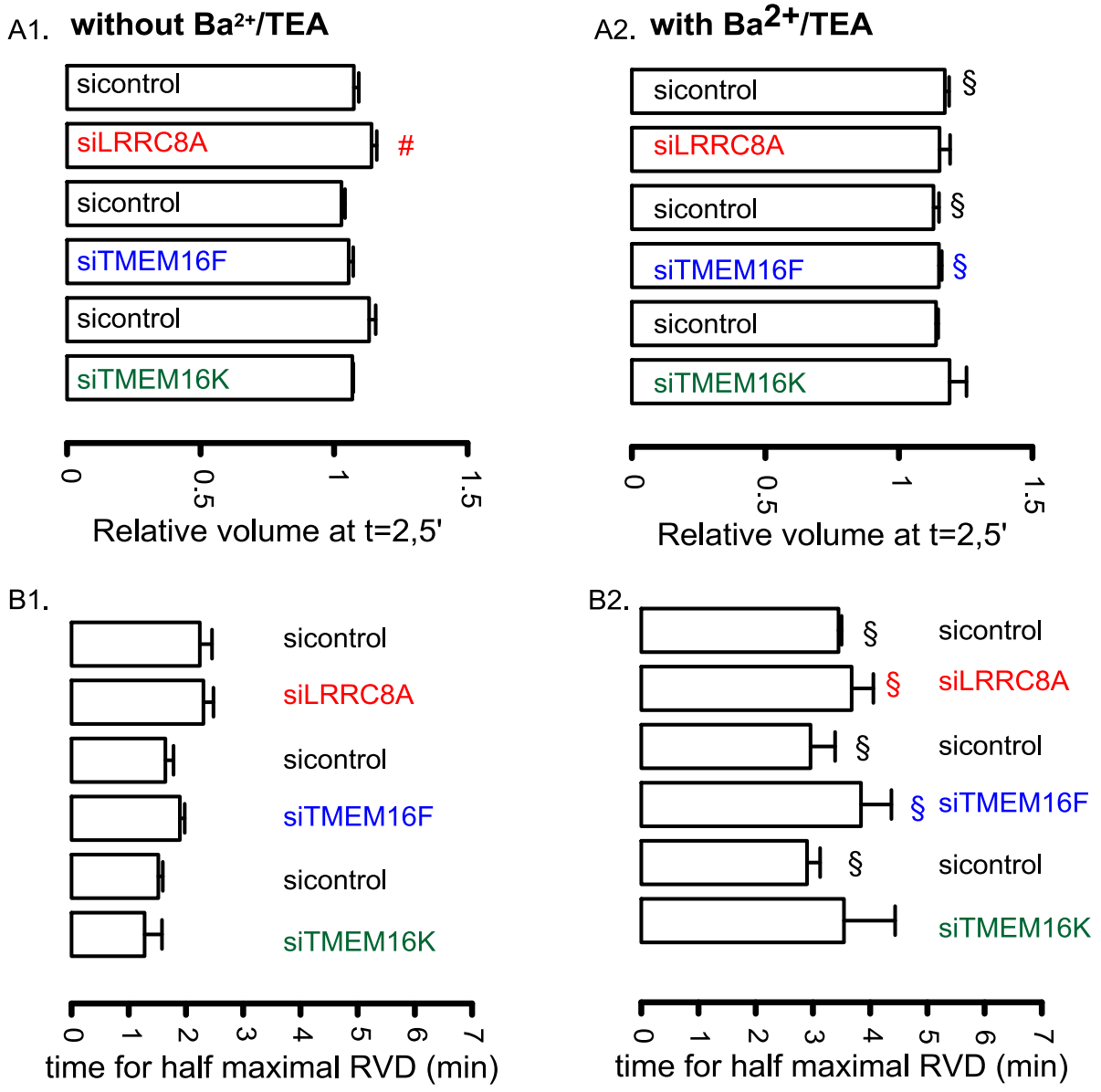

Figure 17: RVD of HeLa cells. A1. Relative volume at t=2,5', in the absence of Ba^{2+}/TEA. # siLRRC8A significantly different to scrambled. A2. Relative volume at t=2,5' in the presence of Ba^{2+}/TEA. § Relative volume significantly different compared to absence of Ba^{2+}/TEA. B1. Time for half maximal RVD in the absence of Ba^{2+}/TEA. B2. Time for half maximal RVD in the absence of Ba^{2+}/TEA. § Time for half maximal RVD significantly different compared to absence of Ba^{2+}/TEA.
Preincubation with Ringer's solution (without or with Ba^{2+}/TEA) before applying Ringer's hypotonic 35% (without or with Ba^{2+}/TEA). Depicted are data for LRRC8A, TMEM16F and TMEM16K deficient cells and the respective sicontrol treated cells for each group. Results given as mean values ± SEM. (Number of experiments is same as in figure 16)

On the contrary, application of the more selective SK3 inhibitor NS 8593 had no effect on the RVD of HeLa cells. Previous experiments have found SK3 channels to be volume sensitive only in hepatic and cholangiocarcinoma cells (Hoffmann et al. 2009) (Fig. 18).

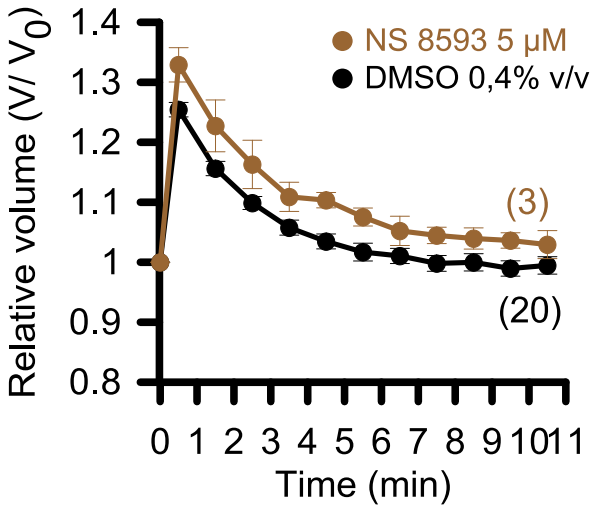

Figure 18: Relative volume against time of NS 8593 and DMSO treated HeLa cells. Preincubation with Ringer's before applying Ringer's hypotonic 35%. Results given as mean volume ± SEM. (Number of experiments).

4.3.8 RVD in HeLa after application of K^+-Cl^- cotransporter inhibitor 2

Even though inhibition of Cl^- and K^+ channels in the previous experiments led to a prolonged RVD, the cells were still able to regulate their volume. In search of a mechanism which had a stronger impact on volume regulation we used the compound RDIOA to inhibit the KCC2. This had indeed a significant effect: a larger relative volume at t=2,5' (1,218 ±0, 010 vs.1,098 ± 0,011), a longer time for half maximal RVD (3,675 ± 0,491 vs. 2,194 ± 0,165 minutes) and a smaller R_0 (0,161 ± 0,073 vs. 0,448 ± 0,028) compared to DMSO (Fig. 19A). In order to further impair the RVD response we applied RDIOA simultaneously to NS 3728. This succeeded to block the RVD in HeLa. The relative volume at t=2,5' (1,208 ± 0,009 vs. 1,098 ± 0,011) and the half maximal RVD (7,5 ± 0,866 vs. 2,194 ± 0,165 minutes) were significantly different compared to DMSO (Fig. 19B). R_0 was not an appropriate criterion for such a flat curve, as it could not be fitted satisfactorily into the equation of exponential decrease.

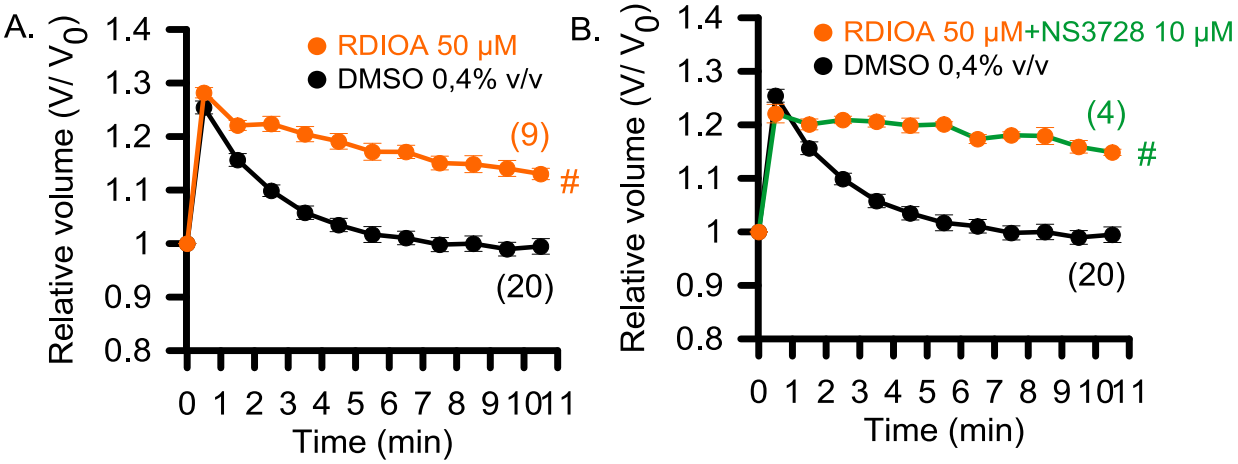

Figure 19: Relative volume against time of inhibitor (closed circle) and DMSO treated (open circle) HeLa cells. Preincubation with Ringer's before applying Ringer's hypotonic 35%. A. RDIOA 50 µM. # Volume at t=2,5', time for half maximal RVD and R0 significantly different to DMSO. B. RDIOA 50 µM + NS 3728 10 µM. # Volume at t=2,5' and time for half maximal RVD significantly different to DMSO. Results given as mean volume ± SEM. (Number of experiments).

4.3.9 RVD in HeLa after application of TRP channel and PI3K inhibitors

As the complex mechanisms of RVD activation and regulation are still not clearly understood, we further investigated the impact of the pharmacological inhibition of the transient receptor potential (TRP) channels and the phosphatidylinositol-4,5-bisphosphate 3-(PI3K) kinases.

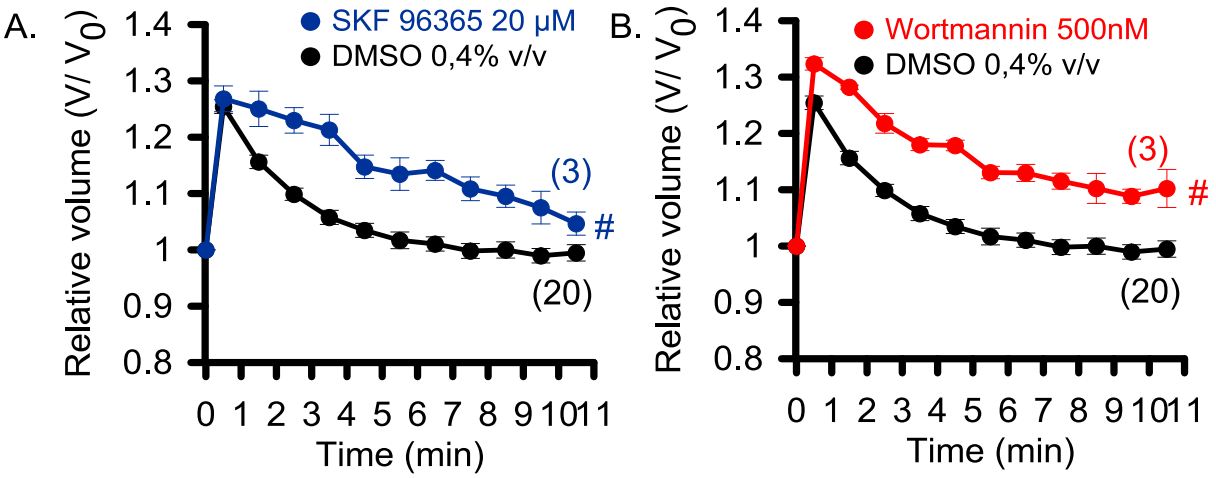

Figure 20: Relative volume against time of inhibitor and DMSO treated HeLa cells. Preincubation with Ringer's before applying Ringer's Hypo 35%. A. SKF 96365 20 µM. # Volume at t=2,5', time for half maximal RVD and R0 significantly different to DMSO. B. Wortmannin 500 nM. # Volume at t=2,5', time for half maximal RVD and R_0 significantly different to DMSO. Results given as mean volume ± SEM. (Number of experiments).

SKF 96365 delayed RVD; the volume at t=2,5' (1,230 ± 0,022vs.1,098 ± 0,011), the time for half maximal RVD (5,273 ± 0,109 vs. 2,194 ± 0,165 minutes) and the R_0 (0,025 ± 0,014 vs. 0,448 ± 0,028) were significantly different compared to DMSO (Fig. 20A).

Wortmannin had a similar effect; the volume at t=2,5' (1,218 ± 0,017 vs.1,098 ± 0,011), the time for half maximal RVD (2,753 ± 0,249 vs. 2,194 ± 0,165 minutes) and the R_0 (0,274 ± 0,034 vs. 0,448 ± 0,028) were also significantly different compared to DMSO (Fig.20B-21).

4.3.10 Summary of RVD parameters for inhibitor treated cells

Volume at t=2,5', R_0, time for half maximal RVD, as well as initial volume at t=0 after incubation with Ringer's control solution for 10 minutes can be seen in Fig. 21 for all compounds used.

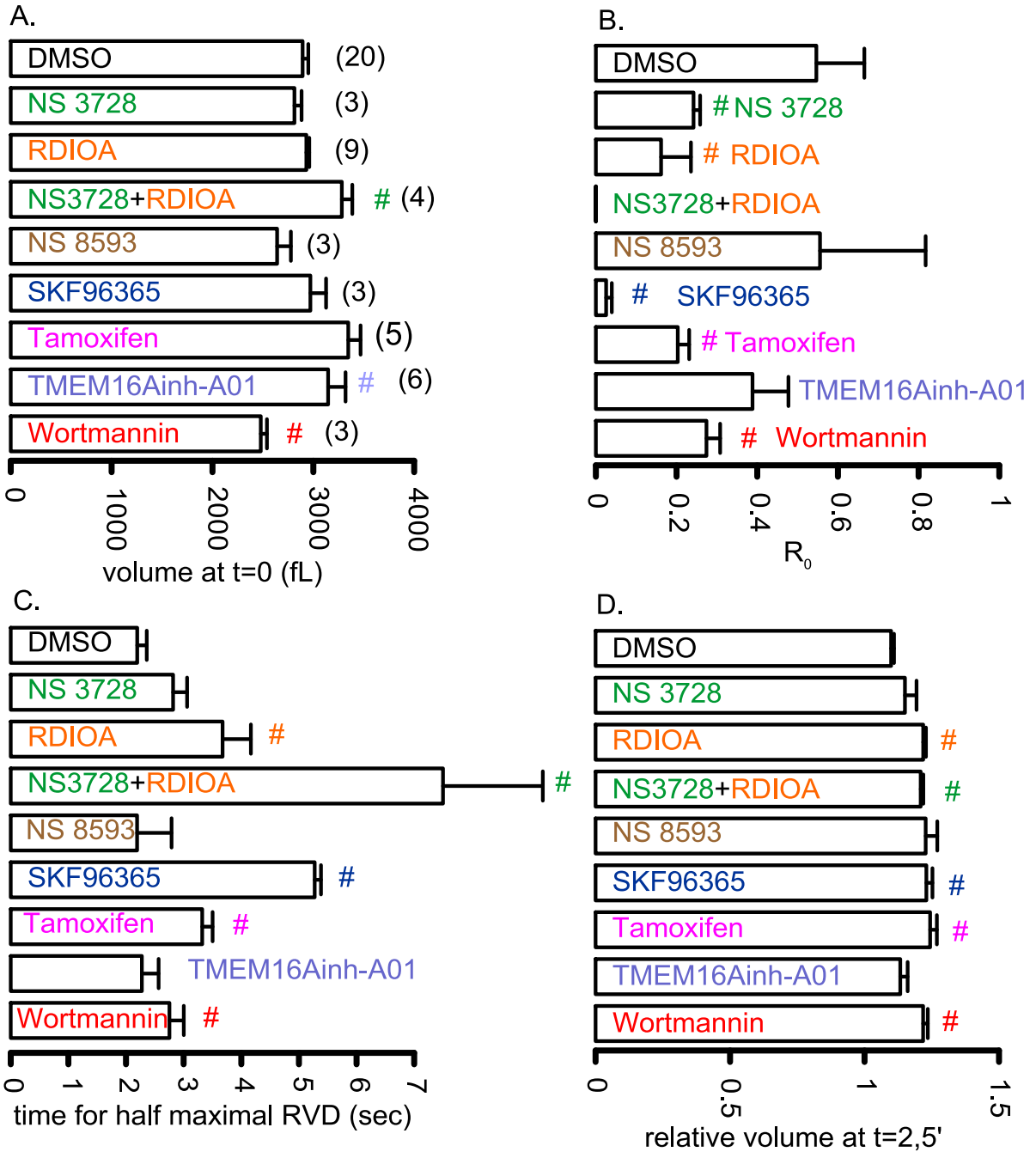

Figure 21: RVD in HeLa cells A. Initial volume at t=0 after incubation with Ringer's control solution for 10 minutes. # significantly different from DMSO. B. R_0. # significantly different from DMSO. C. Time for half maximal RVD. # significantly different from DMSO D. Relative volume at t=2,5' (arbitrary units). # significantly different from DMSO. Results given as mean values ± SEM. (Number of experiments, common in all graphs).

4.3.11 RVD in HeLa after application of staurosporin

VRAC has been linked to AVD and apoptosis. Application of staurosporin on scrambled siRNA treated HeLa cells for 6 hours lead to apoptotic shrinkage and massively compromised the acute RVD as compared to control cells. Practically, staurosporine treated cells no longer showed cell swelling (Fig. 22A). Knockdown of LRRC8A, TMEM16K and application of NS 3728 had no impact on the AVD, whereas the knockdown of TMEM16F and the application of RDIOA could limit cell shrinkage (Fig. 22B).

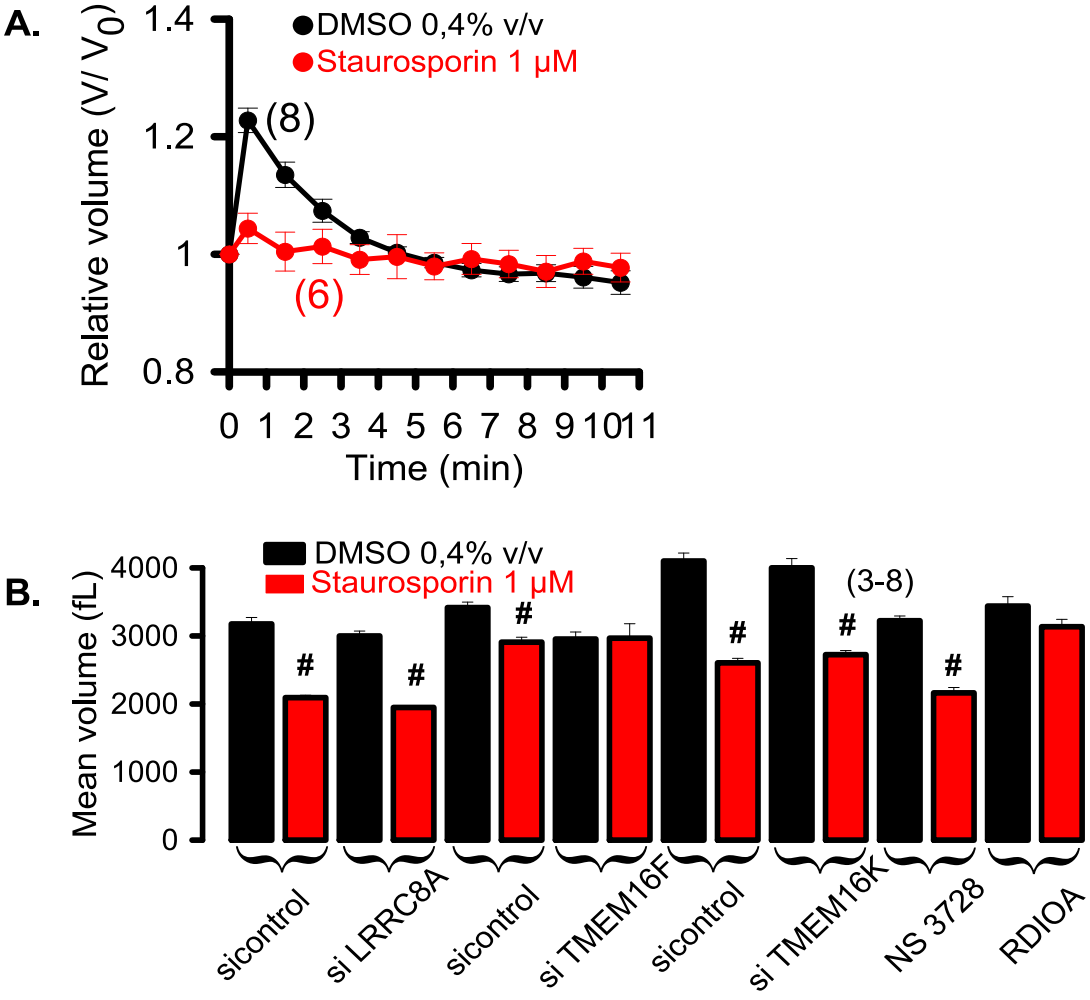

Figure 22: A. Relative volume against time of DMSO and staurosporin treated HeLa cells. Preincubation with Ringer's control solution before applying Ringer's hypotonic 35%. Results given as mean volume ± SEM. B. Mean volume of sicontrol, siLRRC8A, siTMEM16A, siTMEM16F, siTMEM16K, NS 3728 10 µM and RDIOA 50 µM treated HeLa after application of DMSO or staurosporin (Number of experiments). Results given as mean volume ± SEM. # Mean volume significantly lower after treatment with staurosporin compared to treatment with DMSO.

4.4 Apoptosis (Caspase 3) assays

Initially it was essential to determine such a time point for the measurement of the caspase 3 activity, that could show a significant difference in apoptosis rate between DMSO and staurosporin treated cells. This would then allow the detection of possible effects of the inhibitors and siRNA treatments. For this reason, the percentage of the green fluorescent (stained) apoptotic cells to the total of cells was measured every thirty minutes after incubation with caspase 3 substrate with staurosporin 1 μM or DMSO 0,5% v/v in Ringer's solution for a total of six hours (Fig. 24A). An example of caspase 3 activation can be seen in fig. 23.

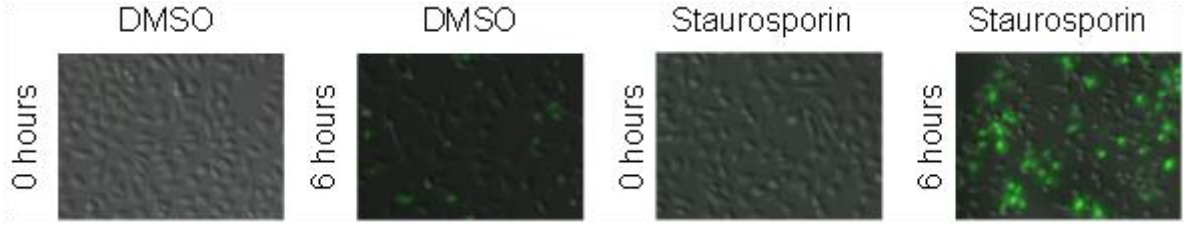

Figure 23: Caspase 3 activity assay at the timepoints of 0 and 6 hours after treatment with DMSO or staurosporin. The green fluorescent cells represent apoptotic cells.

As seen in figure 24A, there is a statistical significance between the rate of the apoptotic cells of the staurosporin treated cells compared to the DMSO treated cells already at t=3,5 hours. At a time point much later than 6 hours the apoptosis induced detaching of a large number of glass. At this single time point the percentage of apoptotic cells after treatment with DMSO was 2,93 ± 0,47% and the percentage of apoptotic dead cells from the cover glass, which could not be counted, a fact which could lead to a biased result (experiment not showed). For these reasons it was deemed necessary to perform the subsequent caspase 3 experiments at the time point of 6 hours, when the difference was quite obvious, but apoptotic cells were still attached to the cover cells after staurosporin treatment was 22,17% ± 1,77%, which is a statistical significant difference (Fig. 24B). The percentage of the apoptotic cells is explicitly higher in this experiment (Fig. 24B) than in the time course experiment for both DMSO and staurosporin treated cells (Fig. 24A, time=6 hours). This could be explained by the exposure of the cover glasses at room temperature and low CO_2 during the time course experiment, when the microscope was used every thirty minutes, compared to the cover glasses of the single time point experiment, which were kept in the incubator for the whole six hours.

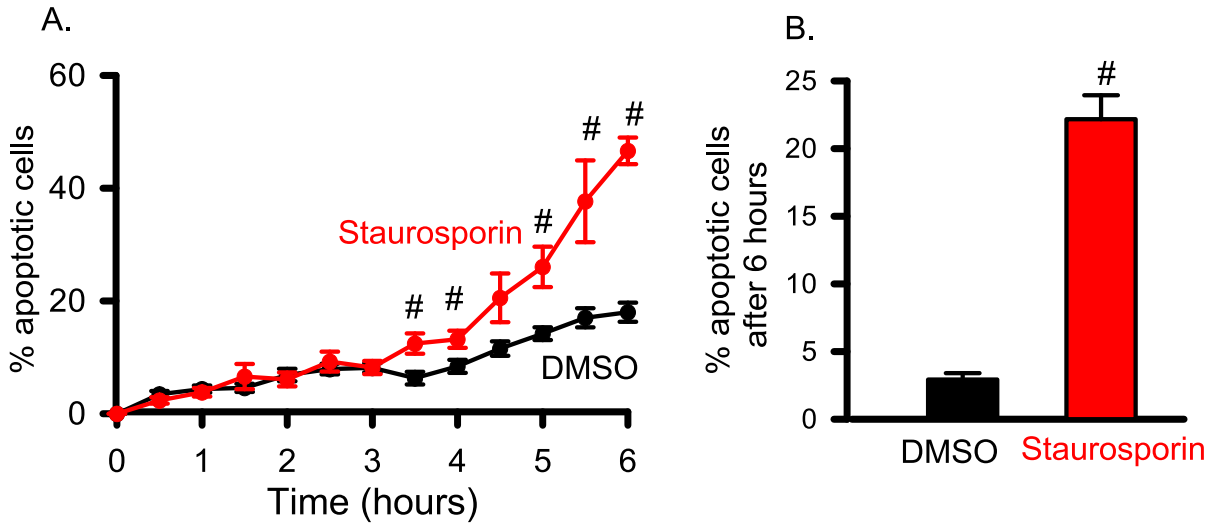

Figure 24: Staurosporin induces apoptosis in HeLa cells. A. Percentage of stained (apoptotic) cells to total cells plotted against time after applying caspase 3 substrate containing staurosporin or DMSO. For time=30 minutes to 4 hours: n experiments=4, n areas ≥ 12. For time= 4,5 - 6 hours: n experiments=1-4, n areas ≥ 3. The difference between DMSO and staurosporin treated cells is already statistically significant according to T-TEST (#) after t=3,5 hours. B. Percentage of the stained cells to total cells examined at a single time point 6 hours after the application of caspase 3 substrate containing DMSO or staurosporin. n experiments=2, n areas = 6. Percentage of apoptotic cells significantly different between staurosporin and DMSO group according to T-TEST(#).The percentage of apoptotic cells for the DMSO group, as well as for the staurosporin group, in experiment A (timepoint:6 hours) and B is statistically different according to T-TEST. Results given as mean values ± SEM.

4.4.1 Induction of apoptosis in the presence of VRAC and KCC inhibitors

As for RVD experiments, NS 3728 was used as a VRAC inhibitor and RDIOA was used as a KCC2 inhibitor. Goal of this experiment was to investigate whether preincubation with NS 3728 or RDIOA had an effect on staurosporin induced apoptosis, compared with preincubation with DMSO. For this reason the experiment was carried out in the groups of DMSO/ staurosporin, NS 3728/ staurosporin and RDIOA/ staurosporin. In order to investigate a possible effect of the inhibitors on apoptosis the control groups of DMSO/ DMSO, DMSO/ NS 3728 and DMSO/ RDIOA were used. The percentage of the apoptotic cells in the DMSO/ DMSO group was 1,72 ± 0,31%, in the DMSO/ staurosporin group 21,26 ± 1,24%, in the NS 3728/ DMSO group 1,31 ± 0,24%, in the NS 3728/ staurosporin 21,27 ± 1,65%, in the RDIOA/ DMSO group 2,66 ± 0,58% and in the RDIOA/ staurosporin group 11,73 ± 0,75%. The results are given as average values ± SEM calculated from the areas/

group. As seen in figure 25, treatment with NS 3728 and RDIOA under control conditions with DMSO 0,5% v/v did not affect the apoptosis rate of the cells. Preincubation with NS 3728 10 µM for thirty minutes before applying staurosporin showed no effect on the apoptosis rate compared to the control group, where the cells were pretreated with DMSO 0,5% v/v. On the contrary, preincubation with RDIOA 50 µM significantly reduced caspase 3 activation.

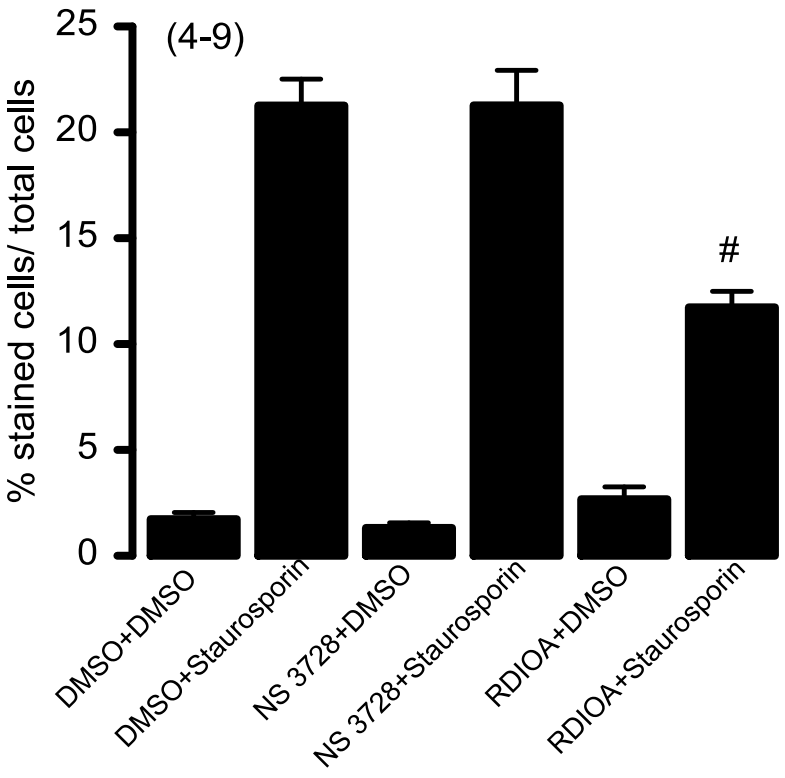

Figure 25: Percentage of the apoptotic/ total cells after treatment with caspase 3 substrate and DMSO/ DMSO, DMSO/ staurosporin, NS 3728/DMSO, NS3728/ staurosporin, RDIOA/ DMSO and RDIOA/ staurosporin. # The RDIOA/ staurosporin treated cells showed a significantly lower apoptosis rate to the control group of DMSO/ staurosporin treated cells. 4-9 cover glasses with a total of 15-40 areas were used/ group. 223-663 cells were examined/ cover glass. Results given as mean values ±SEM.

4.4.2 Induction of apoptosis in LRRC8A and TMEM16F deficient cells

In order to further investigate the role of chloride channels in the AVD and apoptosis, a caspase 3 assay was performed in LRRC8A and TMEM16F deficient cells. The percentage of the dead cells for sicontrol was 21,35 ± 0,80%, for siTMEM16F 17,97 ± 0,71% and for siLRRC8A 15,11 ± 0,72%. The results are given as average values ± SEM calculated from the areas/ group. As seen in figure 26, the knockdown of

TMEM16F and LRRC8A had a statistically significant effect on the caspase 3 activation compared to treatment with control siRNA.

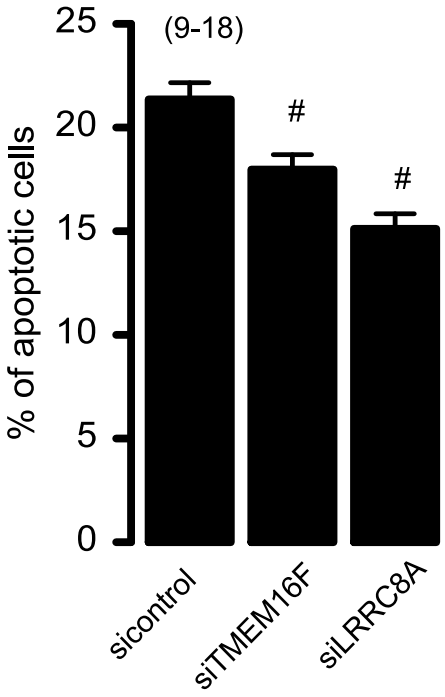

Figure 26: Percentage of the apoptotic/ total cells after treatment with caspase 3 substrate and staurosporin in sicontrol, siTMEM16F and siLRRC8A HeLa cells. Results given as mean values ±SEM. The siTMEM16F and siLRRC8A treated cells both showed a significantly lower apoptosis rate (#) compared to sicontrol. 9-18 cover glasses with a total of 38-67 areas were used/ group. 44-762 cells were examined/ cover glass.

4.5 Proliferation assays in LRRC8A deficient HeLa cells and in the presence of VRAC inhibitors

Given the role of VRAC in apoptosis, it was interesting to examine the proliferation of cells under LRRC8A knockdown and pharmacological inhibition of VRAC. As seen in figure 27, knockdown of LRRRC8A had no effect on the proliferation of HeLa cells within seven days. Application of T16Ainh-A01 10 µM also did not influence the cell numbers. Tamoxifen 1 µM had no significant impact on the cell proliferation. On the contrary, an augmented dose of tamoxifen (10 µM) inhibited proliferation significantly from day 2 to day 7 (Fig. 28).

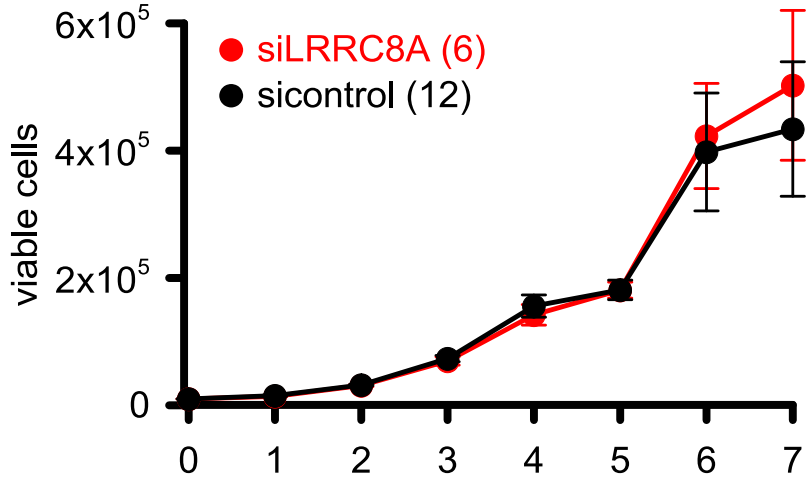

Fig. 27: Viable cells/ well over seven days in sicontrol and siLRRC8A HeLa. Results given as mean values ± SEM. (Number of experiments).

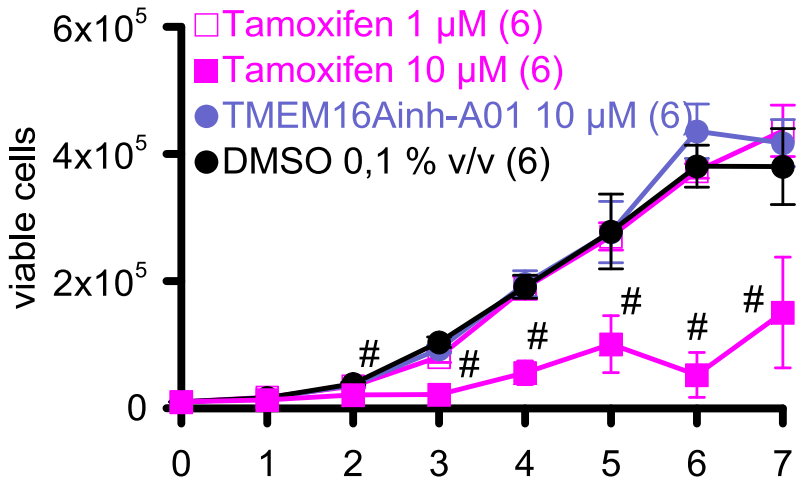

Fig. 28: Viable cells/ well over seven days in presence of DMSO 0,1% v/v, T16Ainh-A01 10 µM, tamoxifen 1 µM and tamoxifen 10 µM. Results given as mean values ± SEM. (Number of experiments). # Under tamoxifen 10 µM significantly different cell numbers from day 2 to day 7.

5. Discussion

VRAC is crucial for RVD and apoptosis. With its molecular identity being unknown for almost thirty years, several proteins have been proposed as candidates. Lately LRRC8A has been recognized as an essential component of the VRAC (Qiu et al. 2014; Voss et al. 2014). The main objective of this study was to examine whether LRRC8A is indispensable for volume regulation. The results of the present work suggest that LRRC8A plays a subsidiary role in RVD of HeLa cells. Flow cytometry experiments in sicontrol HeLa cells demonstrated a completion of the RVD within 5 minutes (Fig.7). After LRRC8A knockdown the RVD was slightly delayed, but was nevertheless completed in a time frame of ten minutes (Fig. 8).

On the contrary, Qiu et al. reported a restoration of cell volume in sicontrol HeLa cells within 20 minutes after the application of hypotonic solution. As to siLRRC8A deficient cells, the relative cell volume was still enlarged up to 1,2 even after 10 minutes. In the experiments of Voss et al. sicontrol human embryonic kidney 293 (HEK) cells did not return to their initial volume even after 60 minutes in hypotonic solution. This is surprising, given that RVD should be quick in order to maintain the fragile cell homeostasis. LRRC8A deficient HEK cells exhibited a total abolition of RVD; relative volume continued to increase even one hour after application of hypotonic solution.

One possible explanation for the inconsistency of these data is the temperature, at which the RVD experiments were performed. The RVD experiments presented here were carried out at 37°C, whereas the experiments in the two papers mentioned above were carried out at room temperature. The channel and transporter activity are both temperature dependent, but energy dependent transporters are more susceptible to low temperature. Low temperature abolished the contribution of KCC to RVD in glia cells, but not the one of Cl^- channels (Ernest et al. 2005). Furthermore, there are remarkable variations among HeLa cells due to occurring mutations in consequence of the very long time that those cells have been in culture (Sun et al. 2015). Passage, cell culture conditions and type may lead to unexpected differences. Transfection is also a factor of variance, with off-target effects being possible. In the

present study one type of siLRRC8A was used, leading to a complete elimination of the protein expression, as proven by immunoblotting (Fig. 5A). In both other studies three and four different pooled siRNAs were used.

In addition, the composition of the isotonic and hypotonic solutions is not unimportant. When developing a protocol for RVD, a major question is how to change only one parameter each time (media→isotonic solution→hypotonic solution), so that the subsequent changes can be clearly attributed to this single change. A common method to create an isotonic and an hypotonic solution for RVD experiments is to use a particular ionic concentration with osmolality lower than 280 mOsm/kg (hypotonic solution) and then add mannitol until an osmolality of 280 mOsm/kg (isotonic solution) is reached. The advantage of this method is that both solutions contain the same ions in the same concentration and only differ in osmolality. This is the reason that this protocol has been broadly used in RVD studies. In this case though, there is a difference in the ionic concentration of Cl^- in the culture medium and the isotonic solution (145 mmol vs. 95 mmol/ L) (Table 3). The reduced extracellular Cl^- concentration causes VRAC activation, as shown by patch clamp recordings of our group, and leads to Cl^- loss, cell shrinkage and a less pronounced cell swelling after application of hypotonic solution. Using this protocol no significant difference was observed in the RVD between LRRC8A deficient and sicontrol HeLa cells (Fig. 8B).

In order to avoid VRAC activation under control conditions we modified the protocol using Ringer's solution without mannitol as a control solution (Cl^- concentration: 145 mmol/ L) (Fig. 29) (Table 3). Under these conditions LRRC8A knockdown lead to a slightly delayed RVD (Fig. 8A). The RVD experiments in BHY cells showed a delayed RVD after LRRC8A knockdown, an effect more pronounced than in HeLa cells (Fig. 10). This is puzzling, given the similar level of the protein expression in immunoblotting (Fig. 5A, 6B). Given that the LRRC8A is an essential component of the VRAC, obviously there are more factors involved in the RVD and the contribution of LRRC8A to RVD in individual cells is rather variable.

TMEM16 are involved in volume regulation and they had been proposed as VRAC candidates in the past (Sirianant et al. 2015; Almaça et al. 2009). In the current series

of experiments HeLa cells do not express TMEM16A and knockdown of TMEM16F and TMEM16K showed no effect on the RVD (Fig. 11).

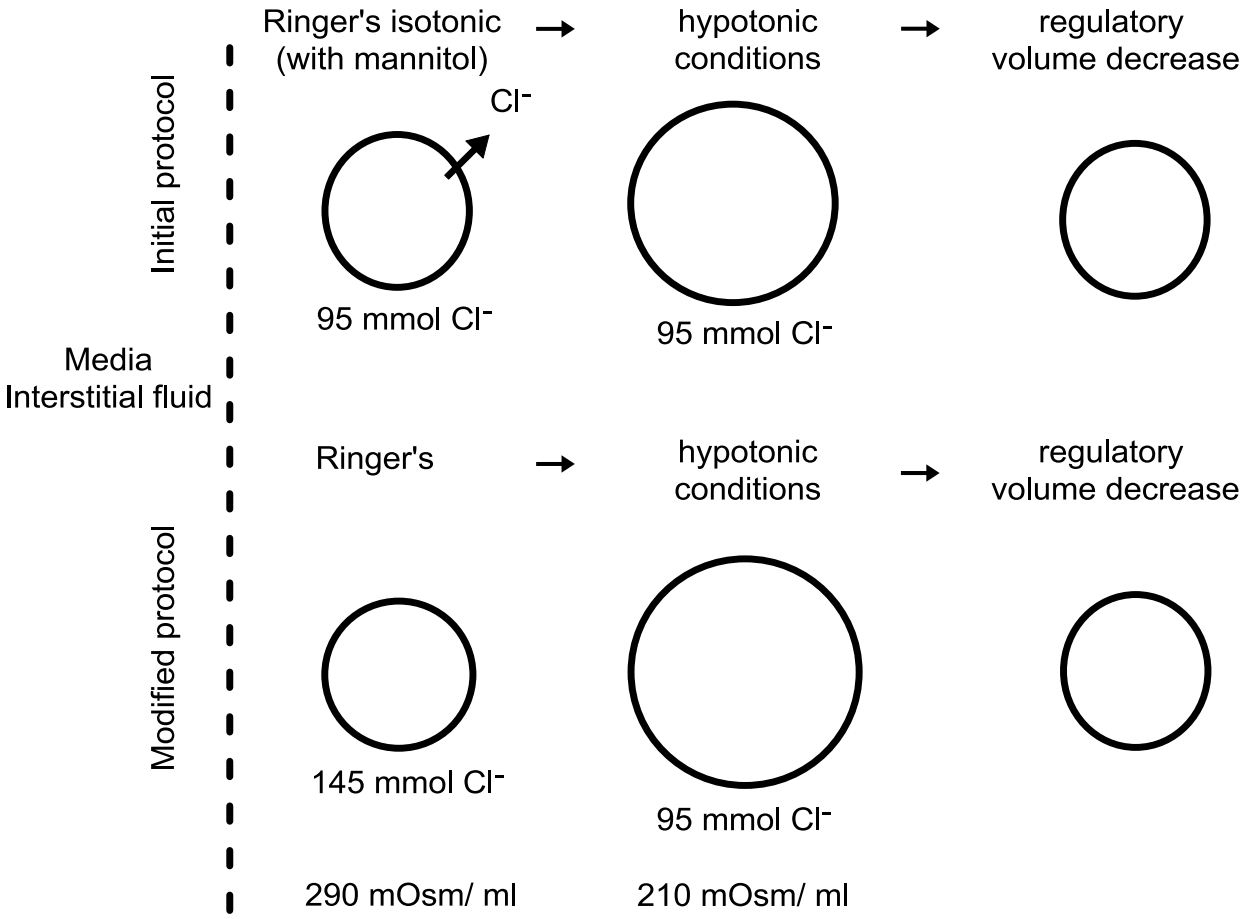

Fig. 29: RVD under two different protocols. Above, using Ringer's isotonic with mannitol as a control solution leads to Cl^- loss in the extracellular space and cell shrinkage. Below, using Ringer's without mannitol and more physiological NaCl concentration, this effect is being avoided.

In previous studies inactivation of TMEM16A in HEK cells has been linked with reduction of the LRRC8A dependent Cl^- current (Sirianant et al. 2014), whereas mice lacking TMEM16A showed impaired $I_{Cl(swell)}$ (Almaça et al. 2009). LRRC8A knockdown had a bigger effect on the RVD in BHY cells, which express TMEM16A abundantly, than in HeLa, which do not express TMEM16A, despite similar levels of LRRC8A expression. The arising question, whether LRRC8A is functionally linked to TMEM16A, should be further investigated in the future.

Even though LRRC8A plays a role in RVD in HeLa cells, volume regulation is still possible after knockdown of LRRC8A, as well as after VRAC inhibition with tamoxifen and NS 3728 (Fig. 13). In comparison, RVD was more attenuated after inhibition of K^+-channels and KCC2. Ba^{2+}/TEA slowed RVD down, whereas the simultaneous knockdown of LRRC8A, TMEM16F and TMEM16K had no additive effect. RDIOA suppressed RVD effectively, suggesting that KCC2 plays a role in the RVD of HeLa cells. The role of KCC for RVD in other cells types, e.g. red blood cells has been demonstrated before (Adragna et al. 2015). In accordance to this, loss of KCC function in cervical cancer cells inhibited cell growth and cancer invasion by impairing volume regulation (Shen et al. 2003). Simultaneous application of RDIOA and NS 3728 had the most pronounced effect.

Even though the VRAC properties have been extensively described, the mechanism of VRAC activation after osmotic swelling is not yet clear. Changes in the intracellular osmolarity have been confirmed as an activating factor, but numerous other mechanisms have been suggested to play a role, for example phospholipase A_2, reactive oxygen species (ROS) and intracellular adenosine triphosphate (ATP) and Ca^{2+} concentration (Kunzelmann 2015). Transient receptor potential (TRP) channels, which serve as sensors for various physical and chemical stimuli, have also been shown to contribute to RVD, by augmenting intracellular Ca^{2+}, which then activates Ca^{2+}-sensitive K^+ and Cl^- channels (Sirianant et al. 2015; Hoffmann und Lambert 2014). Consistent to those data, the TRP channel inhibitor SKF 96365 attenuated RVD in HeLa (Fig. 20A). The PI3K pathway has been also reported to be involved in RVD through mediating taurine efflux (Franco et al. 2004). Its inhibition leads to impaired volume regulation in cardiomyocytes (Wadey et al. 2010). PI3K inhibitor wortmannin also impaired RVD in HeLa (Fig. 20B). As both inhibitors are not perfectly selective, further experiments are necessary to evaluate the role of PI3K and TRP channels in RVD of HeLa.

The involvement of VRAC in the induction of AVD has been well established (Okada et al. 2006; Okada et al. 2004). Under staurosporin HeLa cells exhibited AVD, cell shrinkage and impaired RVD (Fig. 22). Knockdown of LRRC8A had no impact on the proliferation, but could reduce the apoptosis rate after staurosporin. This is consistent

with LRRC8A being an essential component of VRAC. Surprisingly, VRAC inhibition with NS 3728 failed to inhibit both staurosporin induced AVD and caspase activation, a finding which does not agree with previous data (Hoffmann und Lambert 2014). Off target effects of RNA interference or chemical side effects could offer a possible explanation. NS3728 belongs to the relative new group of Cl^- conductance inhibitors of acidic di-aryl ureas, being the most potent of them (Hélix et al. 2003).The structural inhomogenity of the substances that can inhibit VRAC (traditionally: DIDS, niflumic acid, NPPB, tamoxifen and the group of the acidic di-aryl ureas) raise the suspicion that some of these may act by interfering on various levels of the VRAC activation and not directly with the channel (Hélix et al. 2003).

Staurosporin has been shown to activate KCC in erythrocytes (Bize und Dunham 1994). Inhibition of KCC2 with RDIOA could reduce both AVD (Fig. 22) and caspase activation (Fig. 25), to an extent larger than LRRC8A knockdown (Fig.26), implying a role for KCC in AVD in HeLa cells. In previous experiments similar doses of RDIOA did not reduce DNA laddering after staurosporin treatment in HeLa (Okada et al. 2004). This discrepancy could be due to the different methods used. TMEM16F knockdown could also diminish AVD and caspase activation in HeLa cells, confirming its role in apoptosis (Kmit et al. 2013), whereas it had no effect on the RVD.

The LRRC8A gene was first detected in a patient with agammaglobulinemia, lack of B-lymphocytes and minor facial abnormalities which expressed a mutated LRRC8A product along with the normal protein (Sawada et al. 2003). Depletion of the gene in mice lead to increased pre- and postnatal mortality and T-cell dysfunction (Kumar et al. 2014). LRRC8A being an essential VRAC component implies that loss of LRRC8A would have a significant impact on volume regulation, possibly causing a more dramatic phenotype in those animals.

A recent publication claimed that in human retinal pigment epithelial (RPE) cells and in murine sperm cells LRRC8A does not play a role in volume regulation (Milenkovic et al. 2015). The key player in RVD in these tissues was shown to be bestrophin 1 (BEST 1), belonging to a protein family of four paralogues. Human RPE cell lines expressing a mutated BEST1 showed a much smaller $I_{Cl(swell)}$ compared to the control cell line. Knockdown of LRRC8A in the control cell line had no effect on the $I_{Cl(swell)}$

(Milenkovic et al. 2015). Functional disruption of BEST 1 causes retinal macular dystrophy in humans and infertility in mice, possibly as a result of the impaired volume regulation.

In conclusion, LRRC8A plays a role for the RVD of HeLa cells, but volume regulation is still possible without it. LRRC8A contributes to varying degrees to volume regulation among cell types, whereas it does not seem to be involved in AVD. Future research is necessary before LRRC8A could be introduced as a possible pharmacological target.

There are still a lot of aspects which need to be elucidated:

- Do LRRC8A polymers actually form the channel pore?
- How is LRRC8A activated and regulated in detail?
- Are TMEM16 proteins involved?

6. Summary

Volume regulation is a crucial property of all living cells and it contributes to several physiological and pathological procedures. The volume regulated anion channel (VRAC) is involved in volume regulation, more specifically in regulatory volume decrease (RVD), and in volume decrease during apoptosis (apoptotic volume decrease, AVD). The protein LRRC8A (leucin rich repeat protein 8A) has been recently identified as an essential component of VRAC.

In the present study the role of LRRC8A in RVD of HeLa cells could be confirmed using flow cytometry methods. On the other hand, LRRC8A knockdown and pharmacological VRAC inhibition did delay, but did not abolish RVD, showing that other mechanisms, as K^+-Cl^- cotransporters (KCC), play an important role in RVD. In spite of its universal expression, LRRC8A contributes to a various extent to the RVD among cell types. A further goal of this study was to examine whether Ca^{2+} activated chloride channels of the TMEM16 family are involved in RVD. The knockdown of TMEM16F and TMEM16K did not have a direct effect on the RVD of HeLa cells.

HeLa proliferation was not dependent on the presence of LRRC8A. Furthermore, AVD could not be inhibited by LRRC8A knockdown or application of VRAC inhibitors. On the contrary, the present data suggest a role for KCC and TMEM16F in AVD.

7. References

Abascal, Federico; Zardoya, Rafael (2012): LRRC8 proteins share a common ancestor with pannexins, and may form hexameric channels involved in cell-cell communication. In: *Bioessays* 34 (7), S. 551–560. DOI: 10.1002/bies.201100173.

Adragna, Norma C.; Ravilla, Nagendra B.; Lauf, Peter K.; Begum, Gulnaz; Khanna, Arjun R.; Sun, Dandan; Kahle, Kristopher T. (2015): Regulated phosphorylation of the K-Cl cotransporter KCC3 is a molecular switch of intracellular potassium content and cell volume homeostasis. In: *Frontiers in cellular neuroscience* 9, S. 255. DOI: 10.3389/fncel.2015.00255.

Almaça, Joana; Tian, Yuemin; Aldehni, Fadi; Ousingsawat, Jiraporn; Kongsuphol, Patthara; Rock, Jason R. et al. (2009): TMEM16 proteins produce volume-regulated chloride currents that are reduced in mice lacking TMEM16A. In: *J. Biol. Chem.* 284 (42), S. 28571–28578. DOI: 10.1074/jbc.M109.010074.

Antczak, Christophe; Takagi, Toshimitsu; Ramirez, Christina N.; Radu, Constantin; Djaballah, Hakim (2009): Live-cell imaging of caspase activation for high-content screening. In: *J Biomol Screen* 14 (8), S. 956–969. DOI: 10.1177/1087057109343207.

Bize, I.; Dunham, P. B. (1994): Staurosporine, a protein kinase inhibitor, activates K-Cl cotransport in LK sheep erythrocytes. In: *The American journal of physiology* 266 (3 Pt 1), S. C759-70.

Cai, Siyi; Zhang, Tao; Zhang, Dandan; Qiu, Guixing; Liu, Yong (2015): Volume-sensitive chloride channels are involved in cisplatin treatment of osteosarcoma. In: *Molecular medicine reports* 11 (4), S. 2465–2470. DOI: 10.3892/mmr.2014.3068.

Dunham, P. B.; Stewart, G. W.; Ellory, J. C. (1980): Chloride-activated passive potassium transport in human erythrocytes. In: *Proceedings of the National Academy of Sciences* 77 (3), S. 1711–1715. DOI: 10.1073/pnas.77.3.1711.

Elmore, Susan (2007): Apoptosis: a review of programmed cell death. In: *Toxicol Pathol* 35 (4), S. 495–516. DOI: 10.1080/01926230701320337.

Ernest, Nola Jean; Weaver, Amy K.; van Duyn, Lauren B.; Sontheimer, Harald W. (2005): Relative contribution of chloride channels and transporters to regulatory

volume decrease in human glioma cells. In: *American journal of physiology. Cell physiology* 288 (6), S. C1451-60. DOI: 10.1152/ajpcell.00503.2004.

Fadok, V. A.; de Cathelineau A; Daleke, D. L.; Henson, P. M.; Bratton, D. L. (2001): Loss of phospholipid asymmetry and surface exposure of phosphatidylserine is required for phagocytosis of apoptotic cells by macrophages and fibroblasts. In: *The Journal of biological chemistry* 276 (2), S. 1071–1077. DOI: 10.1074/jbc.M003649200.

Franco, Rodrigo; Lezama, Ruth; Ordaz, Benito; Pasantes-Morales, Herminia (2004): Epidermal growth factor receptor is activated by hyposmolarity and is an early signal modulating osmolyte efflux pathways in Swiss 3T3 fibroblasts. In: *Pflügers Archiv : European journal of physiology* 447 (6), S. 830–839. DOI: 10.1007/s00424-003-1211-z.

Hammer, Christian; Wanitchakool, Podchanart; Sirianant, Lalida; Papiol, Sergi; Monnheimer, Mathieu; Faria, Diana et al. (2015): A Coding Variant of ANO10, Affecting Volume Regulation of Macrophages, Is Associated with Borrelia Seropositivity. In: *Molecular medicine (Cambridge, Mass.)* 21, S. 26–37. DOI: 10.2119/molmed.2014.00219.

Han, Qingdong; Liu, Shengwen; Li, Zhengwei; Hu, Feng; Zhang, Qiang; Zhou, Min et al. (2014): DCPIB, a potent volume-regulated anion channel antagonist, attenuates microglia-mediated inflammatory response and neuronal injury following focal cerebral ischemia. In: *Brain research* 1542, S. 176–185. DOI: 10.1016/j.brainres.2013.10.026.

Hazama, A; Okada, Y (J Physiol. 1988 Aug; 402: 687–702.): Ca2+ sensitivity of volume-regulatory K+ and Cl- channels in cultured human epithelial cells.

Hélix, N.; Strøbaek, D.; Dahl, B. H.; Christophersen, P. (2003): Inhibition of the endogenous volume-regulated anion channel (VRAC) in HEK293 cells by acidic di-aryl-ureas. In: *The Journal of membrane biology* 196 (2), S. 83–94. DOI: 10.1007/s00232-003-0627-x.

Hoffmann, Else K.; Lambert, Ian H. (2014): Ion channels and transporters in the development of drug resistance in cancer cells. In: *Philosophical transactions of the*

Royal Society of London. Series B, Biological sciences 369 (1638), S. 20130109. DOI: 10.1098/rstb.2013.0109.

Hoffmann, Else K.; Lambert, Ian H.; Pedersen, Stine F. (2009): Physiology of cell volume regulation in vertebrates. In: *Physiological reviews* 89 (1), S. 193–277. DOI: 10.1152/physrev.00037.2007.

Kerr, J. F.R.; Wyllie, A. H.; Currie, A. R. (1972): Apoptosis: A Basic Biological Phenomenon with Wide-ranging Implications in Tissue Kinetics. In: *Br J Cancer* (August; 26(4)), S. 239–257.

Kida, H.; Miyoshi, T.; Manabe, K.; Takahashi, N.; Konno, T.; Ueda, S. et al. (2005): Roles of aquaporin-3 water channels in volume-regulatory water flow in a human epithelial cell line. In: *The Journal of membrane biology* 208 (1), S. 55–64. DOI: 10.1007/s00232-005-0819-7.

Kmit, A.; van Kruchten, R.; Ousingsawat, J.; Mattheij, N. J. A.; Senden-Gijsbers, B.; Heemskerk, J. W. M. et al. (2013): Calcium-activated and apoptotic phospholipid scrambling induced by Ano6 can occur independently of Ano6 ion currents. In: *Cell death & disease* 4, S. e611. DOI: 10.1038/cddis.2013.135.

Kumar, Lalit; Chou, Janet; Yee, Christina S. K.; Borzutzky, Arturo; Vollmann, Elisabeth H.; Andrian, Ulrich H. von et al. (2014): Leucine-rich repeat containing 8A (LRRC8A) is essential for T lymphocyte development and function. In: *The Journal of experimental medicine* 211 (5), S. 929–942. DOI: 10.1084/jem.20131379.

Kunzelmann, Karl (2015): TMEM16, LRRC8A, bestrophin: chloride channels controlled by Ca(2+) and cell volume. In: *Trends in biochemical sciences. DOI:* 10.1016/j.tibs.2015.07.005.

Lauf, Peter K.; Adragna, Norma C. (2000): K-Cl Cotransport. Properties and Molecular Mechanism. In: *Cellular Physiology and Biochemistry* 10 (5-6), S. 341–354. DOI: 10.1159/000016357.

Lee, Elbert L.; Shimizu, Takahiro; Ise, Tomoko; Numata, Tomohiro; Kohno, Kimitoshi; Okada, Yasunobu (2007): Impaired activity of volume-sensitive Cl- channel is involved in cisplatin resistance of cancer cells. In: *Journal of cellular physiology* 211 (2), S. 513–521. DOI: 10.1002/jcp.20961.

Lentz, Barry R. (2003): Exposure of platelet membrane phosphatidylserine regulates blood coagulation. In: *Progress in Lipid Research* 42 (5), S. 423–438. DOI: 10.1016/S0163-7827(03)00025-0.

Maeno, E.; Ishizaki, Y.; Kanaseki, T.; Hazama, A.; Okada, Y. (2000): Normotonic cell shrinkage because of disordered volume regulation is an early prerequisite to apoptosis. In: *Proceedings of the National Academy of Sciences of the United States of America* 97 (17), S. 9487–9492. DOI: 10.1073/pnas.140216197.

Milenkovic, Andrea; Brandl, Caroline; Milenkovic, Vladimir M.; Jendryke, Thomas; Sirianant, Lalida; Wanitchakool, Potchanart et al. (2015): Bestrophin 1 is indispensable for volume regulation in human retinal pigment epithelium cells. In: *Proc. Natl. Acad. Sci. U.S.A.* 112 (20), S. E2630-9. DOI: 10.1073/pnas.1418840112.

Nilius, B.; Sehrer, J.; Droogmans, G.; (Keine Angabe) (1994): Permeation properties and modulation of volume-activated Cl(-)-currents in human endothelial cells. In: *Br J Pharmacol.* (Aug; 112(4)), S. 1049–1056.

Nilius, Bernd; Prenen, Jean; Voets, Thomas; Eggermont, Jan; Droogmans, Guy (1998): Activation of volume-regulated chloride currents by reduction of intracellular ionic strength in bovine endothelial cells. In: *The Journal of Physiology* 506 (2), S. 353–361. DOI: 10.1111/j.1469-7793.1998.353bw.x.

Okada, Y.; Maeno, E.; Shimizu, T.; Manabe, K.; Mori S.; Nabekura T. (2004): Dual roles of plasmalemmal chloride channels in induction of cell death. In: *Pflugers Arch - Eur J Physiol* (448), S. 287–295. DOI: 10.1007/s00424-004-1276-3.

Okada, Y.; Shimizu, T.; Maeno, E.; Tanabe, S.; Wang, X.; Takahashi, N. (2006): Volume-sensitive chloride channels involved in apoptotic volume decrease and cell death. In: *The Journal of membrane biology* 209 (1), S. 21–29. DOI: 10.1007/s00232-005-0836-6.

Pedersen, S. F.; Klausen, T. K.; Nilius, B. (2015): The identification of a volume-regulated anion channel: an amazing Odyssey. In: *Acta physiologica (Oxford, England)* 213 (4), S. 868–881. DOI: 10.1111/apha.12450.

Picollo, Alessandra; Malvezzi, Mattia; Accardi, Alessio (2015): TMEM16 proteins: unknown structure and confusing functions. In: *Journal of molecular biology* 427 (1), S. 94–105. DOI: 10.1016/j.jmb.2014.09.028.

Qiu, Zhaozhu; Dubin, Adrienne E.; Mathur, Jayanti; Tu, Buu; Reddy, Kritika; Miraglia, Loren J. et al. (2014): SWELL1, a plasma membrane protein, is an essential component of volume-regulated anion channel. In: *Cell* 157 (2), S. 447–458. DOI: 10.1016/j.cell.2014.03.024.

Sawada, Akihisa; Takihara, Yoshihiro; Kim, Ji Yoo; Matsuda-Hashii, Yoshiko; Tokimasa, Sadao; Fujisaki, Hiroyuki et al. (2003): A congenital mutation of the novel gene LRRC8 causes agammaglobulinemia in humans. In: *J. Clin. Invest.* 112 (11), S. 1707–1713. DOI: 10.1172/JCI200318937.

Schreiber, Rainer; Uliyakina, Inna; Kongsuphol, Patthara; Warth, Richard; Mirza, Myriam; Martins, Joana R.; Kunzelmann, Karl (2010): Expression and function of epithelial anoctamins. In: *The Journal of biological chemistry* 285 (10), S. 7838–7845. DOI: 10.1074/jbc.M109.065367.

Shen, Meng-Ru; Chou, Cheng-Yang; Hsu, Keng-Fu; Hsu, Yueh-Mei; Chiu, Wen-Tai; Tang, Ming-Jer et al. (2003): KCl cotransport is an important modulator of human cervical cancer growth and invasion. In: *The Journal of biological chemistry* 278 (41), S. 39941–39950. DOI: 10.1074/jbc.M308232200.

Sirianant, Lalida; Ousingsawat, Jiraporn; Tian, Yuemin; Schreiber, Rainer; Kunzelmann, Karl (2014): TMC8 (EVER2) attenuates intracellular signaling by Zn2+ and Ca2+ and suppresses activation of Cl- currents. In: *Cellular signalling* 26 (12), S. 2826–2833. DOI: 10.1016/j.cellsig.2014.09.001.

Sirianant, Lalida; Ousingsawat, Jiraporn; Wanitchakool, Podchanart; Schreiber, Rainer; Kunzelmann, Karl (2015): Cellular volume regulation by anoctamin 6: Ca(2+), phospholipase A2 and osmosensing. In: *Pflugers Archiv : European journal of physiology. DOI:* 10.1007/s00424-015-1739-8.

Skommer, Joanna; Darzynkiewicz, Zbigniew; Wlodkowic, Donald (2014): Cell death goes LIVE. Technological advances in real-time tracking of cell death. In: *Cell Cycle* 9 (12), S. 2330–2341. DOI: 10.4161/cc.9.12.11911.

Sørensen, Belinda Halling; Thorsteinsdottir, Unnur Arna; Lambert, Ian Henry (2014): Acquired cisplatin resistance in human ovarian A2780 cancer cells correlates with shift in taurine homeostasis and ability to volume regulate. In: *American journal of physiology. Cell physiology* 307 (12), S. C1071-80. DOI: 10.1152/ajpcell.00274.2014.

References

Springer Medizin Verlag (Hg.) (2007): Physiologie des Menschen mit Pathophysiologie. 30. Auflage. Unter Mitarbeit von Robert F. Schmidt und Florian Lang. Heidelberg.

Stutzin, A.; Hoffmann, E. K. (2006): Swelling-activated ion channels: functional regulation in cell-swelling, proliferation and apoptosis. In: *Acta physiologica (Oxford, England)* 187 (1-2), S. 27–42. DOI: 10.1111/j.1748-1716.2006.01537.x.

Sun, Han; Chen, Chen; Lian, Baofeng; Zhang, Menghuan; Wang, Xiaojing; Zhang, Bing et al. (2015): Identification of HPV integration and gene mutation in HeLa cell line by integrated analysis of RNA-Seq and MS/MS data. In: *Journal of proteome research* 14 (4), S. 1678–1686. DOI: 10.1021/pr500944c.

Suzuki, Jun; Umeda, Masato; Sims, Peter J.; Nagata, Shigekazu (2010): Calcium-dependent phospholipid scrambling by TMEM16F. In: *Nature* 468 (7325), S. 834–838. DOI: 10.1038/nature09583.

Tian, Yuemin; Schreiber, Rainer; Kunzelmann, Karl (2012): Anoctamins are a family of Ca2+-activated Cl- channels. In: *J. Cell. Sci.* 125 (Pt 21), S. 4991–4998. DOI: 10.1242/jcs.109553.

Verhoven, B. (1995): Mechanisms of phosphatidylserine exposure, a phagocyte recognition signal, on apoptotic T lymphocytes. In: *Journal of Experimental Medicine* 182 (5), S. 1597–1601. DOI: 10.1084/jem.182.5.1597.

Voss, Felizia K.; Ullrich, Florian; Münch, Jonas; Lazarow, Katina; Lutter, Darius; Mah, Nancy et al. (2014): Identification of LRRC8 heteromers as an essential component of the volume-regulated anion channel VRAC. In: *Science (New York, N.Y.)* 344 (6184), S. 634–638. DOI: 10.1126/science.1252826.

Wadey, R.; Howell, S.; Brook, T.; Hall, S.: PI3Kinase signalling is instrumental in cardiac cell volume regulation. In: *Proc Physiol Soc 19, PC106* 2010.

Wehner, F.; Olsen, H.; Tinel, H.; Kinne-Saffran, E.; Kinne, R. K. H. (2003): Cell volume regulation: osmolytes, osmolyte transport, and signal transduction. In: *Reviews of physiology, biochemistry and pharmacology* 148, S. 1–80. DOI: 10.1007/s10254-003-0009-x.

Yang, Huanghe; Kim, Andrew; David, Tovo; Palmer, Daniel; Jin, Taihao; Tien, Jason et al. (2012): TMEM16F forms a Ca2+-activated cation channel required for lipid

scrambling in platelets during blood coagulation. In: *Cell* 151 (1), S. 111–122. DOI: 10.1016/j.cell.2012.07.036.

As part of this work the following article has been submitted for publication:

Sirianant, Lalida; Podchnart, Wanitchacool; Ousingsawat, Jiraporn; Benedetto, Roberta; Zormpa, Anna; Cabrita, Ines, Schreiber, Rainer, Kunzelmann, Karl. (2015): Volume regulation without LRRC8A.

8. Acknowledgements

Firstly, I would like to express my sincere gratitude to my advisor Prof. Dr. Kunzelmann for giving me the chance to work in his laboratory in the first place and for his continuous support during the whole time of this work. His deep knowledge of physiology, his patience and his unstoppable, infectious enthusiasm were a great inspiration and motivation. Beyond scientific knowledge, seeing unanswered questions, complications and unexpected results as a challenge rather than a problem, was the most important lesson that I have been taught by him.

Besides my advisor, I would like to thank Prof. Dr. Schreiber, for the intensive everyday support, considering both practical matters and theoretical questions, as for the RNA isolation. My sincere thanks also goes to Dr. Ousingsawat for the introduction to research methods, her steady helpfulness and constructive advice.

HeLa cells were kindly provided by Prof. Dr. Karin Hoppe-Seyler (German Cancer Research Center, Heidelberg) and the BHY cells were a gift from Dr. Christian Ruiz (Institute of Pathology, University Clinic, Basel).

I thank my fellow lab mates Lalida Sirianant, Roberta Benedetto and Ines Cabrita for their help, advice, fertile exchange of ideas and for all the fun (in and outside the lab!). I specially thank Podchanart Wanitchacool for performing the western blots.

I also thank Brigitte Wild, Ernestine Tartler and Patricia Seeberger for their precious technical and moral support.

9. Curriculum vitae

For reason of data protection, the Curriculum vitae is not published in the electronic version.